Norbornene-dicarboximide Based Copolymers for Electro-optic Application

アリサ, バンナロン

KYUSHU UNIVERSITY

Norbornene-dicarboximide Based Copolymers

for Electro-optic Application

Interdisciplinary Graduate School of Engineering Sciences

Kyushu University

ALISA BANNARON

2020

Dear coffee and of spirit…

Contents

CHAPTER III

Norbornene-dicarboximide (NDI) Based Monomers and Electro-optic (EO) Polymers ... - 40 -

CHAPTER V

Abstract

Electro-optic (EO) polymers have been continuously utilized in optical devices for decades due to their advantageous properties over traditional LiNbO$_3$. Especially, larger EO coefficient larger r_{33} over 100 pm/V from organic materials which enables optical devices to achieve ultra-fast transmission for future generation communication. Moreover, high compatibility of EO polymer, also allows efficient integration with other optical components, leading to advancement in performance of optical devices. Therefore, EO polymers have become major building blocks for unique and powerful platform using in several sophisticated optoelectronic applications.

Since then, several polymeric hosts have been applied to improve thermos-physical properties to accomplish temporal stability for long-term usage. The most widely used polymer as a host is poly(methyl methacrylate) (PMMA). However, post-polymerisation approach to achieve final PMMA based EO polymeric product is considered as time and solvent consuming method as it requires large amount of organic solvent for purification. To shorten this process, in this work, we applied norbornene-dicarboximide (NDI) derivatives as a polymeric backbone for EO polymers. Series of side-chain NDI based EO copolymers were synthesized by ring opening metathesis polymerisation (ROMP). By using mild ruthenium-based catalyst, Grubbs 3$_{rd}$ generation (G3), allowed polymerisation to undergo pre-polymerisation approach, in which the final EO polymer could be obtained by one-pot synthesis. Variety of EO chromophore loading density, side groups, as well as hydrocarbon spacer between NDI backbone and EO chromophore were varied to study thermos-physical properties of NDI polymers, which would be appropriate as EO polymers.

In-situ r33 measurement of NDI based EO polymers were preliminarily measured by Teng-Man refraction technique at the wavelength of 1310 nm. The selective EO polymer was later fabricated into A hybrid polymer Mach-Zehnder EO modulator and ultra-thin silicon with 50 μm thick and 3 μm wide. The modulator showed excellent $V_\pi \bullet L$ product at 1.90 V$\bullet$cm at poling temperature 150°C.

In short, the simplicity in synthesis of NDI based polymer by one-pot approach shows potential perspective for fabrication of EO modulator in optoelectronic application. In addition, high thermal stable and well-controlled NDI polymer also allowed improvement in physical properties for EO polymers. This could be practically applied to large-scale production for commercial manufacturer.

Preface

Data communication has been the key matter of our world since 19th Century to transmit data from sender to receiver through medium for a distance. Since then, advancement in data exchange technologies have been rapidly growing to fulfill human beings in any aspects. In the early stage, wires were selected as transmitted backbone for nationwide framework. Varieties of wire designs were utilized to overcome limitation of capability, as well as bandwidth. However, numbers of obstacles including high losses at high frequencies, and was the major constraint, until the next breakthrough was the utilization of single mode optical fiber which rely the interface of two important technologies, electronics and photonics. This integrated technology has brought the progress to another level by providing large information capacity, small transmission losses, as well as low heat generation.

The phenomenon occurring from this particular platform is nonlinear optics (NLO) which is relevant to the interaction of high intensity light with matter. Nonlinear optics thus have been a rapid growing concept to widen variety of applications ranging from optical information processing, sensors, data storages *etc*. This photonic integrated circuit includes several interesting aspects of electronic revolution including NLO materials, microfabrication, as well as chip-scale design circuits that allow possibility of cheap large-scale manufacture.

The scope of this thesis is a plethora of topics, including the background theory, material syntheses, optimization and characterizations, as well as the fabrication of EO polymer-based modulator.

The thesis is structured as follows; In **Chapter I**, the fundamental of nonlinear optic phenomenon based on *Maxwell's equation* is firstly introduced, following by the principle of *Pockels effect* in order to understand the relation between external electrical field and change in refractive index of materials. Then, major types of EO materials, inorganic and organic, are also described in comparison. Moreover, brief introduction of Mach-Zehnder interferometer (MZI) and the induction of second-order nonlinearity of EO materials are covered

In **Chapter II**, we clarify all chemicals and instrumentals used in this dissertation. All experimental setups and methods for syntheses are also provided.

Chapter III involves the brief introduction of general polymer systems utilized as EO polymers. Then, thermal-physical characterizations of NDI monomers and NDI based EO polymers by NMR, GPC, DSC, and UV-Vis spectrometer are discussed. The optimization to achieve well-balanced between physical, thermal, and optical properties is also investigated.

Chapter IV is focused on the measurement of *in-situ* r_{33} of NDI based EO polymers by Teng-Man technique at 1310 nm as well as the fabrication of selective NDI based EO polymer into Mach-Zehnder EO modulators and measurement of half-wave voltage at wavelength 1550 nm.

Chapter V is the summary the main results of this dissertation. It also includes the prospect of using novel NDI based EO polymer for EO modulation in industry and an outlook for future work.

CHAPTER I

Theoretical Background

This chapter consists of theoretical background of applications and materials involved in this study and is structured as follows;

1.1 Nonlinear Optics (NLO) Phenomenon

For understanding of nonlinear optics (NLO) phenomenon occurring in photonic devices, such as optical waveguides and modulators, polarised light is considered to be electromagnetic wave. Hence, *Maxwell's equation* is used to realise nonlinear behavior of polarised light and to analyse impact of this polarisation on the propagating light in different dielectric materials [1], [2];

$$\nabla X E(r,t) = -\frac{\partial B(r,t)}{\partial t} \tag{1-1}$$

$$\nabla X H(r,t) = J(r,t) + \frac{\partial D(r,t)}{\partial t} \tag{1-2}$$

$$\nabla . D(r,t) = \rho(r,t) \tag{1-3}$$

$$\nabla B(r,t) = 0 \tag{1-4}$$

where **E***(r,t)* is electric field, **H***(r,t)* is magnetic field, **B***(r,t)* is magnetic induction, **J***(r,t)* is current density and ρ*(r,t)* is charge density in three-dimensional space **r = (x, y, z)**т. **D***(r,t)* is electric displacement current which can be described by;

$$D(r,t) = \varepsilon_0 E(r,t) + P(r,t) \tag{1-5}$$

where ε_0 is vacuum electric permittivity and **P***(r,t)* indicates polarisation in which depends on local value of electric field **E**.

The electric polarisation can be differently explained to **P***(r,t)* = **P**L*(r,t)* + **P**NL*(r,t)*, which **P**L*(r,t)* is linear polarisation that depends on very low electric field **E** and is expressed by;

$$P^L(r,t) = \varepsilon_0 \chi E(r,t) \qquad \text{(1-6)}$$

However, since the coherent high intensity light source is applied, **P**NL*(r,t)* is an extended term representing nonlinear polarisation. Polarisation becomes field independent, while the susceptibility becomes field dependent. As a result, the total polarisation **P** expansion can be expressed in term of electric field **E** in more general relation as follow;

$$P_{tot}(r,t) = \varepsilon_o \{\chi^{(1)} E(r,t) + \chi^{(2)} E^2(r,t) + \chi^{(3)} E^3(r,t) + \cdots \qquad \text{(1-7)}$$

where $\chi^{(1)}$ denotes linear susceptibility for linear optical properties of materials such as refractive index η, dispersion, birefringence, and absorption. $\chi^{(2)}$ and $\chi^{(3)}$ are representing nonlinear susceptibilities in 2nd and 3rd orders, respectively. However, since the scope of this thesis is mainly focused on 2nd order nonlinearity for electro-optic modulators, $\chi^{(3)}$ will be neglected here.

$\chi^{(2)}$ is a quadratic term which is responsible for *second harmonic generation (SHG)* phenomenon, firstly observed by Franken et al., since 1961 [3], [4]. SHG is a frequency-doubling process, where two waves with the same frequencies, ω_1 and ω_2 (where $\omega_1 = \omega_2$),

travelling through nonlinear optical medium, and consequently generate a polarised wave with double frequency $2\omega_d$, see **Figure 1.1**.
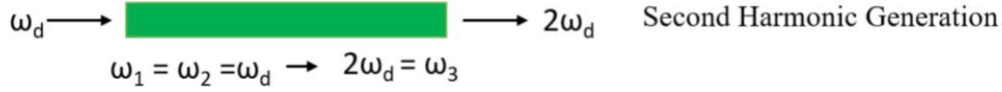
Figure 1.1 Schematic illustration representing SHG phenomenon

Next, the phenomenon occurring through the nonlinear optical materials (medium), so called *electro-optic (EO) effect* will be discussed.

1.2 Principle of Electro-optic (EO) or Pockels Effect

NLO is a process involving the alter of optical frequency through the nonlinear materials (medium), which takes place by linearly changing its refractive index η under the presence of electric field **E**. The particular effect, producing a variation of refractive index, is called *electro-optic (EO)* or *Pockels effect*, which is a result of second order nonlinear interaction between low-frequency electric field with $\omega_0 \approx 0$ and a high-frequency optical field ω_c in a material with second-order susceptibility $\chi^{(2)}$ tensor. Thus, the second-order nonlinear polarisation can be written as [5];

$$P_i(\omega_c \approx \omega_c + \omega_0) = 2\varepsilon_0 \sum_{jk} \chi^{(2)}_{ijk}(\omega_c + \omega_0)E_j(\omega_c)E_k(\omega_o \approx 0) \qquad (1\text{-}8)$$

where the indices *i,j,k* denote three orthogonal coordinate axes.

This phenomenon simply has been exploited to create building-block for ultra-fast optical modulators in telecommunication.

In the following, the Einstein notation for sums is used with **Eq.** (1-8) to express the displacement field spectrum $D_i(\omega)$ as;

$$D_i(\omega_c) = \varepsilon_0 \left(\delta_{ij} + \chi_{ij}^{(1)}(\omega_c) \right) E_j(\omega_c) + 2\varepsilon_0 \chi_{ijk}^{(2)}(\omega_c + \omega_0) E_j(\omega_c) E_k(\omega_0) \qquad (1\text{-}9)$$

As low-frequency field is defined as;

$$\varepsilon_{ij} = \varepsilon_0 \left(\delta_{ij} + \chi_{ij}^{(1)} + 2\chi_{ijk}^{(2)} E_k(\omega_0) \right) = \varepsilon_0 (\varepsilon_{r,ij} + \Delta\varepsilon_{r,ij}) \qquad (1\text{-}10)$$

The nonlinear change of the permittivity $\Delta\varepsilon_r$ is given by;

$$\Delta\varepsilon_{r,ij} = 2\chi_{ijk}^{(2)} E_k(\omega_0) \qquad (1\text{-}11)$$

The nonlinear perturbation Δn of refractive index $n + \Delta n$, which is proportional to slowly varying electric field **E,** is approximated as;

$$\varepsilon_r + \Delta\varepsilon_r = (n + \Delta n)^2 \approx n^2 + 2n\Delta n \qquad (1\text{-}12)$$

where second-order susceptibility $\chi_{ijk}^{(2)}$ is often referred in term of electro-optic (EO) coefficient r_{ijk} as related in;

$$r_{ijk} = -\frac{2\chi_{ijk}^{(2)}}{n^4} \qquad (1\text{-}13)$$

Therefore, the change of refractive index under applied electric field can be expressed by;

$$\Delta n_{ij} = -\frac{1}{2} n^3 r_{ijk} E_k(\omega_0) \qquad (1\text{-}14)$$

However, when permutation symmetry of the fields is considered, the independent components of the tensors $\chi^{(2)}$ and r are reduced. Therefore, the tensor components can be contracted to use only two indices, $\chi_{ih}^{(2)}, r_{ih}$, where h is referred to jk and is described by following substitutions;

$$
\begin{array}{ll}
\textbf{1} \text{ for } jk = 11, & \textbf{2} \text{ for } jk = 22 \\
\textbf{3} \text{ for } jk = 33, & \textbf{4} \text{ for } jk = 23 \text{ or } 32 \\
\textbf{5} \text{ for } jk = 13 \text{ or } 31, & \textbf{6} \text{ for } jk = 12 \text{ or } 21
\end{array}
\qquad (1\text{-}15)
$$

1.3 Second-order Nonlinear Materials

Nonlinear optical (NLO) materials play an important role on future generation information technology and industry, where the progress is extremely dependent on development of excellent NLO materials. In this subsection, two types of NLO materials that demonstrate bulk EO coefficient r_{33} in relationship with optical properties in microscopic scale.

1.3.1 Inorganic Crystal: Lithium Niobate (LiNbO$_3$)

As mentioned before, the mechanism that allow SHG phenomenon to occur is EO effect which is the reaction between beams and NLO material as a medium under electric field. LiNbO$_3$, a ferroelectric material firstly discovered in 1949, had been a significant material for fabrication of EO modulators in early stage [6]. This is due to its combination of high optical transparency in near infrared (NIR) wavelength used for telecommunications, EO coefficient, and stability operation over range of temperature (1100 °C – 1180 °C) [7], [8]. In spite of progress toward LiNbO$_3$ modulators, its performance, however, is restricted by a variety of physical obstacles.

The major issue of the particular inorganic crystal is large dielectric constant which often results in optical-electrical velocity mismatch (walk-off) at high frequencies [9]. Moreover, Nagata et al. has found problematic reliability of Ti:LiNbO3 modulator due to its large pyroelectric effect that caused thermal and DC drift on wafers [10].

1.3.2 Organic Electro-optic (OEO) Materials (Chromophores)
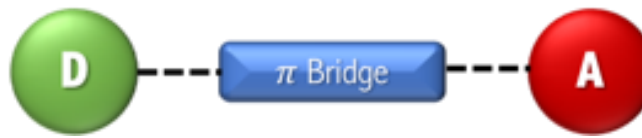
Figure 1.2. Illustration of organic electro-optic (OEO) materials

In general, organic electro-optic (OEO) materials or chromophores, are designed chemical molecules consist of an electron donor (D), electron acceptor (A) which are linked by an extended π-conjugated bridge (DπA system), see **Figure 1.2**. This structure allows electron delocalization of from appropriate donor to acceptor under applied electric field, which resulting as induction of dipole moment [11]. The microscopic nonlinear dipole moment of OEO molecule can be expressed in term of power series;

$$p_i = \mu_i + \alpha_{ij}E_j + \beta_{ijk}E_jE_k + \gamma_{ijkl}E_jE_kE_l + \cdots \qquad (1\text{-}16)$$

where p_i is molecular polarisability, μ is electric dipole moment resulting of electron delocalisation, α is first-order polarisability, β is the second-order polarisability (second hyperpolarisability), and γ is the third-order polarisability. The indices $i,j,k = (x,y,z)$ represents orthogonal coordinate axes of the molecule, z axis is the axis of the dipole moment. Most importantly, β denotes hyperpolarisability which is the second-order nonlinearity in

microscopic scale. Since NLO chromophores are usually possessed along dipole axis *z*, therefore, the hyperpolarisability is demonstrated as β_{zzz} which can be expressed by [12];

$$\beta_{zzz} \propto \frac{\Delta\mu_{eg}(\mu_{ge})^2}{E_{ge}^2} \qquad (1\text{-}17)$$

where $\Delta\mu_{eg}$ indicates the difference in diploe moment between the highest occupied (HOMO) and the lowest unoccupied (LUMO) molecular orbitals, μ_{ge} is the transition dipole moment (oscillator strength) and E_{ge} is energy difference between ground state (HOMO) and charge transfer excited state (LUMO).
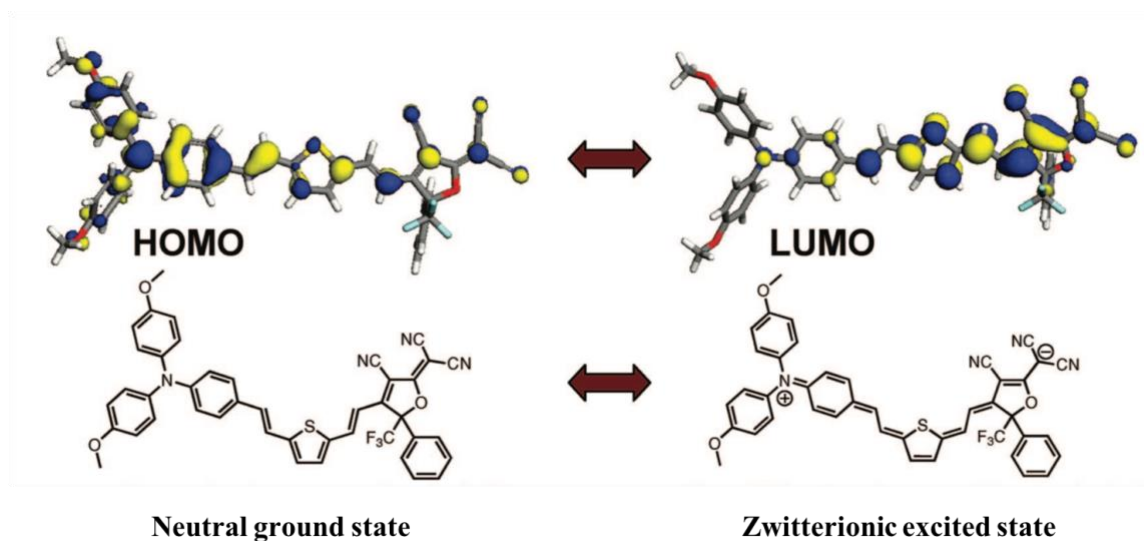
Figure 1.3. Density functional theory (DFT) computer modeling generated electron density surface depiction of HOMO and LUMO of a triaryl amine donor/tricyanovinylfuran acceptor EO chromophore and chemical structure depiction of the EO chromophore at ground and Zwitterionic Mulliken charge transfer excited states [12].

β_{zzz} is relevant to the second-order susceptibility as;

$$\chi^{(2)}_{333} = Ng\langle cos^3\theta\rangle\beta_{zzz} \qquad (1\text{-}18)$$

N (molecule/cm3) is the number density of the active nonlinear molecules that interact with the incident optical filed. g is the Lorentz-Onsager local field factor. $\langle cos^3\theta\rangle$ is the average acentric parameter implying the extent of NLO chromophore alignment with respect to applied external field. θ is an angle between external field, in which align to axis 3, and dipole moment axis z (**Figure 1.4**).
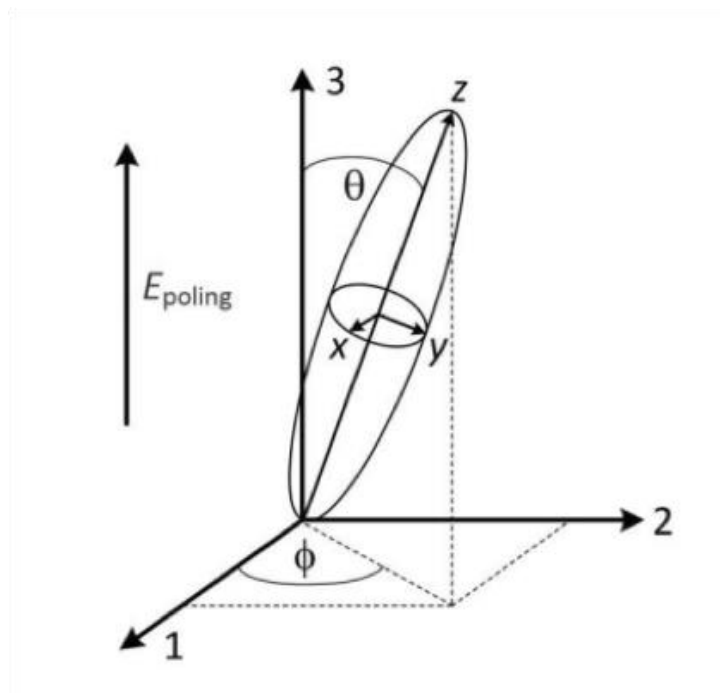
Figure 1.4. Orientation of the molecular coordinate system (*x,y,z*) with respect to the global coordinate system (*1,2,3*). The ellipsoid represents the NLO molecule and z axis is the dipole moment axis. The external poling field E$_{poling}$ is applied along axis 3, forcing molecular dipole moment to align along axis 3 [5].

Therefore, by substituting **Eq.** (1-18) onto **Eq.** (1-13), the macroscopic linear EO efficient r_{33} is given by;

$$r_{33} = \frac{-2\chi_{333}^{(2)}}{n_0^4} = -2N\beta_{zzz}\langle cos^3\theta\rangle\frac{g}{n_0^4} \qquad (1\text{-}19)$$

In summary, the efficiency of organic NLO materials significantly depends on the microscopic EO polarisability β_{zzz}, number density of dipoles, as well as the alignment of average EO chromophores with respect to poling field, E_{poling}. These factors can be molecularly designed by engineering molecular structure of donor, acceptor, and π-conjugated bridge.

In comparison with LiNbO$_3$, OEO materials have intrinsically proven advantageous characteristics such as high bandwidth over 100 GHz, low dielectric constant ε ≈ 2.5 – 4.0, low dispersion and high compatibility towards the integration with numbers of optical components [13], [14]. Most importantly, organic EO chromophore could be assembled into large EO coefficient that, in turn, permits π-phase shift achieving digital level. Therefore, numbers of organic EO materials have been intensively investigated for decades with several approaches [15]-[18].

Table 1.1 shows the summary comparison between LiNbO$_3$ and electro-optic (EO) materials which is practically incorporated into polymer matrix for physical property. EO polymer systems will be later discussed in detail in Chapter III.

Property	LiNbO₃	EO polymers
EO coefficient, r_{33} (pm/V)	30-33	≥ 100
Dielectric constant, ε	28	$2.5 - 4.0$
Refractive index, η	2.2	$\sim 1.6 - 1.7$
Optical loss (dB/cm)	0.2	$0.2 - 1.1$
Cost	Relatively high	Low
Integration	Difficult	Relatively easy

Table 1.1 General comparison between LiNbO₃ and EO polymers

1.4 Mach-Zehnder Interferometer (MZI)
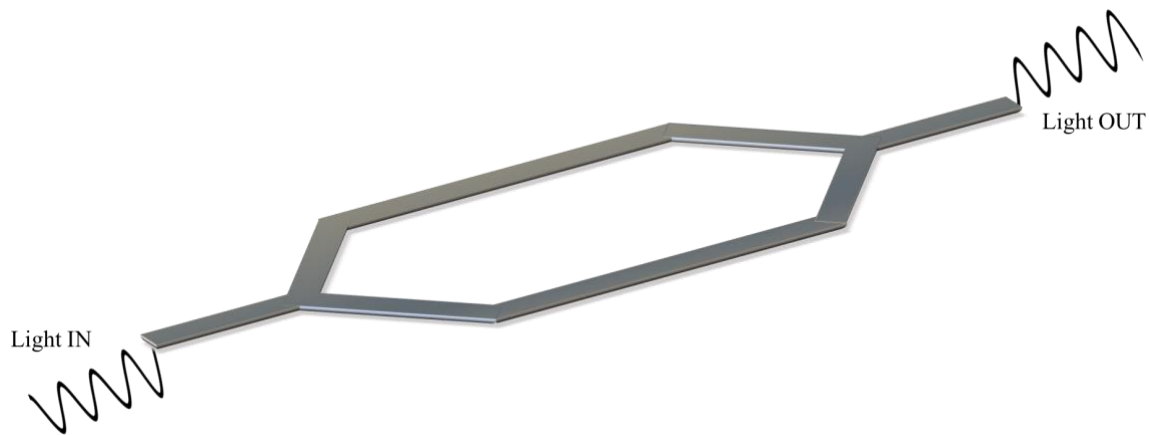
Figure 1.5 Simple Mach-Zehnder interferometer (MZI) waveguide

The Mach-Zehnder interferometer (MZI) (see **Figure 1.5**) was originally proposed by Ernst Mach and Ludwig Zehnder in 1891. [19] It is a simple prototype stripline device for demonstrating interference by amplitude, mostly used as modulator for the external optical modulation. An input light beam in single mode is firstly split into two parts at the beam-splitter (Y-junction) and later recombined at the second beam-splitter.

The voltage required to achieve complete wave modulation is called *half-wave voltage (V$_\pi$)* as given by;

$$V_\pi = \frac{\lambda d}{2\eta^3 r_{33} L \Gamma}$$

(1-20)

where λ is an optical wavelength, d is the electrode gap, L is the electrode length (interaction length of the electrical and optical fields), and Γ is an overlap integral between electrical and optical fields.

Typically, MZI waveguides are fabricated from an EO materials in which exhibiting EO effect or Pockels effect as discussed in section 1.2. Pockels effect is an EO activity in macroscopic level which can be achieved by the alignment of EO chromophores into non-centrosymmetry. This particular procedure is so called *poling process*.

1.5 Induction of EO activity by electric poling process
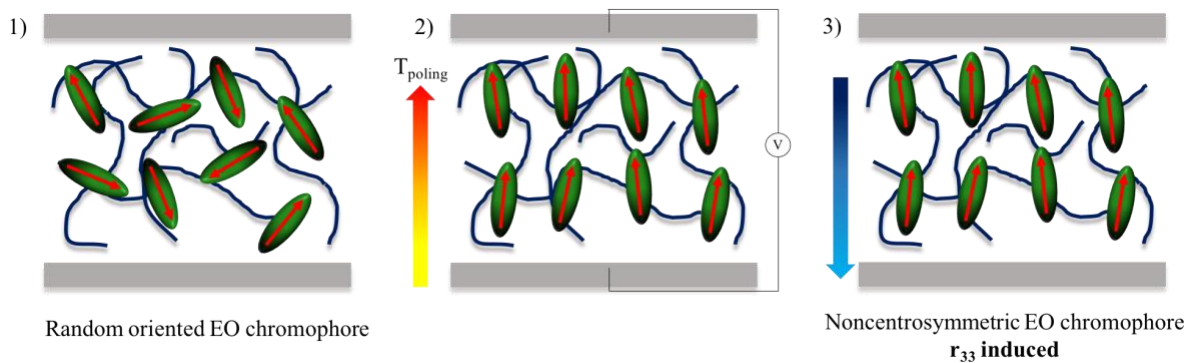
Figure 1.6 Schematic illustration of the electric poling process

Poling is the material processing to induce EO activity in molecular level into macroscopic level, r_{33} as described in **Eq.** (1-19). The most common configuration is contact electrode poling, where EO material is casted into thin film between two electrodes in direct contact. This is because it may also be used as the driving electrodes for completed EO devices. The methodology is started by heating the film close to its glass transition temperature (T_g), so called T_{poing}. This process would allow the dipole molecules to increase their mobility. Subsequently, an electric field is applied across two electrodes to force the rotation of EO chromophores toward electric field axis. After short period of time, the temperature is then decreased below T_g to freeze the alignment. After poling processing, the bulk material is invariant under rotations along poling axis, providing second order nonlinearity. [12]

1.6 Measuring EO coefficient of poled EO polymers

For decades, EO polymers have received appreciable attention for optical devices due to large EO coefficient as a result of its flexibility of molecular engineering. In this section, general methods for determination of EO coefficient (r_{33}) will be discussed.

1.6.1 Teng-Man technique

There are several techniques exist for measurement of the relevant bulk material EO coefficients, such as Teng-Man method, attenuated total reflection (ATR), and two-slit interference. Among these, Teng-Man method is the most widely used due to its simple configuration (see **Figure 1.7**) since it is noncontact technique requiring only optics and low-power diode lasers. [12] In addition, the sample is simply prepared by spin-coating EO polymer onto indium tin oxide (ITO) glass, which is served as one of two electrodes, following by fabrication of Au electrode on top. This apparatus works by *in-situ* monitoring EO response (change in refractive index) as a function of time-varying input polarisation. The change in

phase angle results in an output intensity modulation when the light is passed through a polarizer. The intensity change is proportional to r_{33} as follow;

$$r_{33} = \frac{3\lambda I_m}{4\pi V_m I_c n^2} \frac{(n^2 - sin^2\theta)^{3/2}}{(n^2 - 2sin^2\theta)} \frac{1}{sin^2\theta} \approx \frac{I_m}{I_c} \tag{1-21}$$

where I_m is the amplitude of modulation, V_m is the modulation voltage across EO polymer film, I_c is half maximum intensity, and n is the refractive index of the EO polymer. [20]-[22]
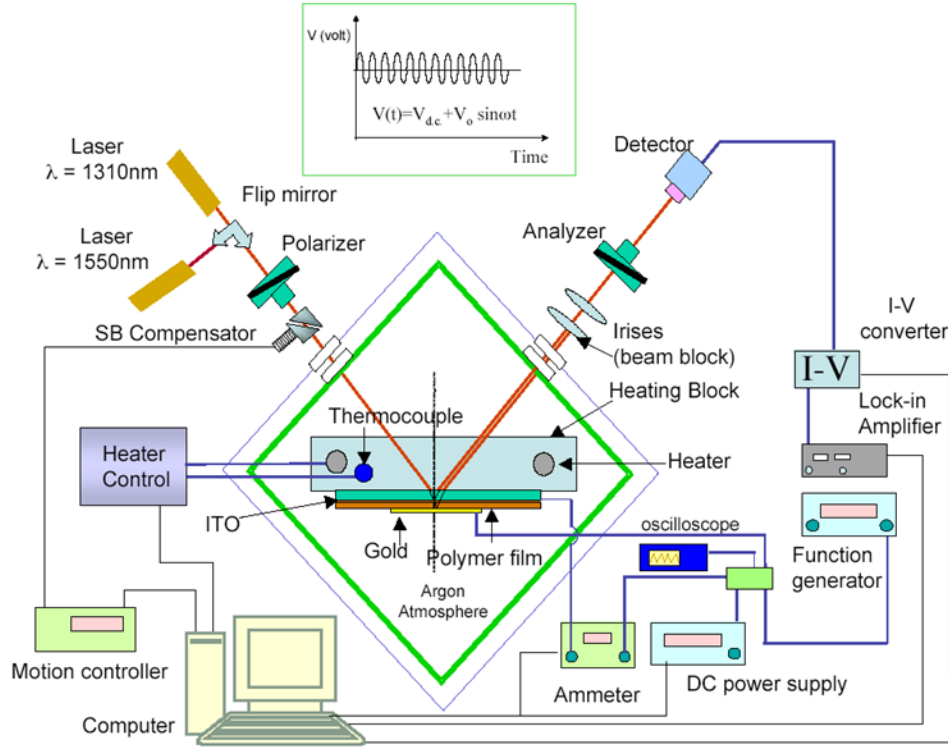
Figure 1.7 Schematic illustrator of Teng-Man apparatus

However, the *in-situ* r_{33} determined by this technique is practically measured only at the wavelength of 1.3 μm. This is to prevent inaccurate complication from multiple reflections caused by refractive index contrast at interfaces in the multilayer sample. [23]

1.6.2 Fiber-optic Mach-Zehnder interferometer
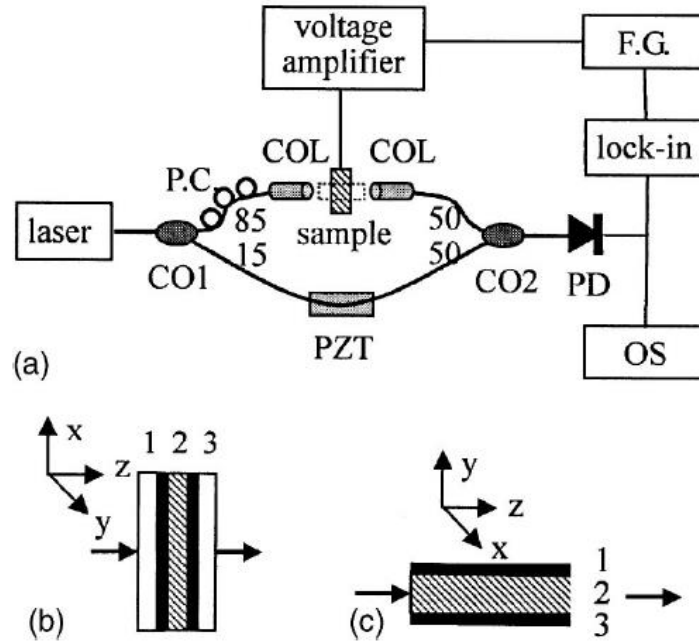
Figure 1.8 (a); fiber-optic MZI measurement setup, (b); polymer thin film sample, and (c); polymeric waveguide sample (1, 2, and 3 indicate upper electrode, polymer waveguide, and lower electrode, respectively) [24]

Characterisation of r_{33} using MZI apparatus involves fabrication of poled polymeric waveguide, which consisting of lower and upper cladding layers. In comparison to Teng-Man technique, this method is more attractive as it is the measurement of device's performance (*in-device r_{33}*) which is relevant to half-wave voltage (V_π) as depicted in **Eq.** 1-20, thus it is considered to be more accurate. Moreover, continuous light excitation is employed in this alternative.

1.7 Thesis's Motivation and Objective

Over decades, the tremendous development in telecommunication industry in their rules and structures has completely changed the interaction of humanity across the world. It becomes the significant segment of people's everyday lives. Therefore, the traffic of internet of things (IoT) is calling for the advancement to increase the capability of transmission, while being friendly to environment by reducing its energy consumption.

This thesis, thus, reviews the substantial theories and progress of nonlinear optical materials, which would enable the understanding of basic concepts in utilization of EO materials with well-designed platforms to achieve another level of telecommunication. Since the quality of optical materials significantly affects the performance of the application, therefore, the development of EO materials is also challenging growth in the industry.

The EO modulator is one of the promising building blocks inside the device for optical communication, which in fact, has been exponentially growing in the current microwave photonics and fiber-optic networks. Among several types of materials used in the devices, *EO polymers* show outstanding advantages such as large EO coefficient, low dielectric constant and loss, and excellent compatibility for integration with other optical components, which overall leading to remarkable performance in terms of high data rate, low power consumption, as well as well compatibility with circuit system.

However, the practical reliability issue of organic based EO polymers has always been questioned. This is due to the thermally structural relaxation of acentric alignment of EO materials during operation, when heat is commonly generated. Therefore, highly thermal

stability of EO polymer has to be essentially investigated to meet commercially environmental standard.

Herein, we purpose the use of novel polymeric host, norbornene-dicarboximide (NDI), due to its distinctive thermal and physical properties to be utilized as active materials in EO modulators. We studied the properties of NDI polymer ranging from its syntheses, thermos-physical characterization and optimization, as well as the fabrication into EO polymer-based modulators. Moreover, we expect to simplify synthetic preparation of EO polymers such as solvent and time consumption. In order to expand the probability of employing NDI based polymer into commercial level.

Bibliography

[1] C. Koos, Nanophotonic Devices for Linear and Nonlinear Optical Signal Processing, Karlesruhe Series in Photonics & Communications.

[2] A. Dakshanamoorthy, "Fundamentals of nonlinear optical materials," *PRAMANA — journal of physics,* vol. 57, pp. 871-883, 2001.

[3] P. A. Franken, A. E. Hill, C. W. Peters, and G. Weinreich, "Generation of Optical Harmonics," *Physical Review Letters,* vol. 7, pp. 118-119, 1961.

[4] S. Suresh, A. Ramanand, D. Jayaraman, and P. Mani, "Review on Theoretical Aspect of Nonlinear Optics," *Reviews on Advanced Materials Science ,* vol. 30, pp. 175-183, 2012.

[5] R. Palmer, Silicon Photonic Modulators for Low-power Applications, KIT Scientific Publishing.

[6] I. P. Kaminow and J. R. Carruthers, "Optical Waveguiding Layers in $LiNbO_3$ and $LiTaO_3$," *Applied Physics Letter,* vol. 22, pp. 326-328, 1973.

[7] R. S. Weis and T. K. Gaylord, "Lithium Niobate: Summary of Physical Properties and Crystal Structure," *Applied Physics A,* vol. 37, pp. 191-203, 1985.

[8] Ed L. Wooten, K. M. Kissa, A. Yi-Yan, E. J. Murphy, D. A. Lafaw, P. F. Hallemeier, D. Maack, D. V. Attanasio, D. J. Fritz, G. J. McBrien and D. E. Bossi, "A Review of Lithium Niobate Modulators for Fiber-Optic Communications Systems," *IEEE JOURNAL OF SELECTED TOPICS IN QUANTUM ELECTRONICS,* vol. 6, pp. 69-82, 2000.

[9] S. K. Korotky, G. Eisenstein, R. S. Tucker, J. J. Veselka, and G. Raybon, "Optical Intensity Modulation to 40 GHz Using a Waveguide Electrooptic Switch," *Apply Physics Letter,* vol. 50, no. 23, pp. 1631-1633, 1987.

[10] H. Nagata and J. Ichiwaka, "Progress and Problems in Reliability of Ti:LiNbO$_3$ Optical Intensity Modulators," *Optical Engineering,* vol. 34, pp. 3284-3293, 1995.

[11] J. L. Oudar and D. S. Chemla, "Hyperpolarizabilities of the nitroanilines and their relations to the excited state dipole moment," *The Journal of Chemical Physics,* vol. 66, pp. 2664-2668, 1977.

[12] L. R. Dalton, P. A. Sullivan, and D. H. Bale, "Electric Field Poled Organic Electro-optic Materials: State of the Art and Future Prospects," *Chemical Reviews,* vol. 110, pp. 25-55, 2010.

[13] B. A. Block, T. R. Younkin, P. S. Davids, M. R. Reshotko, P. Chang, B. M. Polishak, S. Huang, J. Luo, A. K.-Y. Jen, "Electro-optic Polymer Cladding Ring Resonator Modulators," *Optics Express,* vol. 16, pp. 18326-18333, 2008.

[14] A. K.-Y. Jen, J. Luo, T.-D. Kim, B. Chen, S.-H. Jang, et al, "Exceptional Electro-optic Properties Through Molecular Design and Controlled Self-assembly," in *Proceedings of SPIE*, Sandiego, 2005.

[15] S. R. Marder, D. N. Beratan, L.-T. Cheng, "Approaches for Optimizing the First Electronic Hyperpolarizability of Conjugated Organic Molecules," *Science,* vol. 252, pp. 103-106, 1991.

[16] S. R. Marder, C. B. Gorman, B. G. Tiemann, and L.-T. Cheng, "Stronger Acceptors Can Diminish Nonlinear Optical Response in Simple Donor-Acceptor Polyenes," *Journal of the American Chemical Society,* vol. 115, pp. 3006-3007, 1993.

[17] T. Verbiest, S. Houbrechts, M. Kauranen, K. Clays, and A. Persoons, "Second-order Nonlinear Optical Materials: Recent Advances in Chromophore Design," *Journal of Materials Chemistry,* vol. 7, pp. 2175-2189, 1997.

[18] P. A. Sullivan and L. R. Dalton, "Theory-Inspired Development of Organic Electro-optic Materials," *Accounts of Chemical Research,* vol. 43, pp. 10-18, 2010.

[19] A. K. Majumdar and J. C. Ricklin, Free-Space Laser Communications: Principle and Advance, Springer, 2010.

[20] C. C. Teng and H. T. Man, "Simple reflection technique for measuring the electro-optic coefficient of poled polymers," Applied Physics Letters, vol. 56, pp. 1734-1736, 1990.

[21] Y. Shuto and M. Amano, "Reflection measurement technique of electro-optic coefficients in lithium niobate crystals and poled polymer films," Journal of Applied Physics, vol. 77, pp. 4632-4638, 1995.

[22] S. Prorok, A. Petrov, M. Eich, J. Luo, and A. K.-Y. Jen, "Modification of a Teng-Man technique to measure both r_{33} and r_{13} electro-optic coefficients," Applied Physics Letters, vol. 105, p. 113302, 2014.

[23] D.-H. Park, C.-H. Lee, and W. N. Herman, "Analysis of multiple reflection effects in reflective measurements of electro-optic coefficients of poled polymers in multilayer structures," Optics Express, vol. 14, pp. 8866-8884, 2006.

[24] Y.-P. Wang, J.-P. Chen, X.-W. Li, J.-X. Hong, X.-H. Zhang, J.-H. Zhou, and A.-L. Ye, "Measuring electro-optic coefficients of poled polymers using fiber-optic Mach–Zehnder interferometer," Applied Physics Letters, vol. 85, pp. 5102-5103, 2004.

CHAPTER II

Materials, Instrument, and Experimental

This dissertation discusses both EO polymeric syntheses and its performance as EO modulator. Therefore, in this chapter, all chemical materials involved in synthesis of EO polymers, characterization methods, and fabrication for particular devices will be summarised.

2.1 Materials

Table 2.1 includes all chemical materials and their sources of commercial manufacturers for purchase, listed in order of use.

Chemicals	Purchased sources
Maleic anhydride	Tokyo Chemical Industry
O-dichlorobenzene	Kanto Chemical
Dicyclopentadiene	Kanto Chemical
Monochlorobenzene	Kanto Chemical
Cyclohexylamine	Kanto Chemical
Hexylamine	Tokyo Chemical Industry
Triethylamine	Tokyo Chemical Industry
β-alanine	Kanto Chemical
4-aminobutyric acid	Kanto Chemical
5-aminovaleric acid	Tokyo Chemical Industry
6-aminohexanoic acid	Kanto Chemical
7-aminoheptanoic acid	Tokyo Chemical Industry
Pyridine	Tokyo Chemical Industry
Acetic anhydride	Kanto Chemical
Sodium acetate	Kanto Chemical

N-(*3*-dimethylaminoproply)-*N'*-ethylcarbodiimide hydrochloride (WSC)	Nacalai Tesque
4-dimethylaminopyridine (DMAP)	Tokyo Chemical Industry
Monomethyl-*5*-norbornene-*2,3*-dicarboxylate	Tokyo Chemical Industry
Grubbs 3rd generation catalyst (G3)	Sigma Aldrich
Ethyl vinyl ether (EVE)	Kanto Chemical
Dichloromethane	Tokyo Chemical Industry
Cyclopentanone	Kanto Chemical
1,2-dichloroethane	Kanto Chemical
o-dichlorobenzene	Kanto Chemical

Table 2.1 List of chemicals and purchased manufacturers.

2.2 Instrument

Characterizations for molecular structures were performed using Nuclear Magnetic Resonance (NMR) spectroscopy (Nihon Denshi JEOL JNM-LA400 spectrometer at 400 MHz) using deuterated $CDCl_3$ or DMSO with tetramethylsilane (TMS) as an internal standard. High resolution mass spectrometry (HRMS) used in this thesis was Nihon Denshi JEOL MStation JMS700. The molecular weights and polydispersity of EO polymers were measured by Gel Permeation Chromatography (GPC) that separates analytes on the basis of size using Shodax GPC K-804L column on a JASCO LC2000 liquid chromatography system, in THF as an eluent. Glass transition temperature (T_g) was determined by Differential Scanning Calorimetry (DSC) using Seiko Instruments Inc SII-DSC 6220, under nitrogen atmosphere at heating rate 10°C/min. Decomposition temperature (T_d) was carried out by Thermogravimetric Analysis (TGA), Seiko Instruments Inc SII-TG/DTA 6200 instrument, under nitrogen atmosphere at the heating rate 10°C/min. UV absorption spectra were observed on Shimadzu UV-Vis spectrometer 1240 with standard concentration 5mg/100 ml THF.

2.3 Experimental

2.3.1 Synthesis of precursor (1)
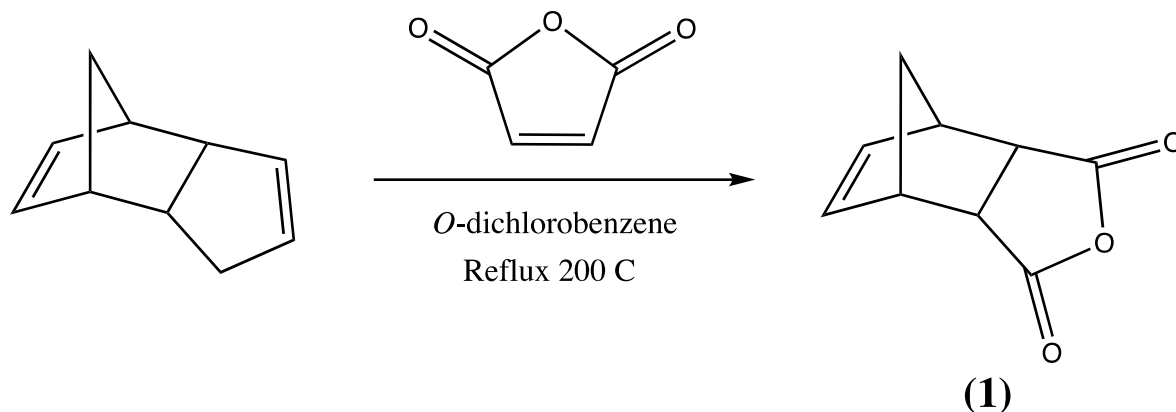
Figure 2.1 Synthetic scheme of precursor (1)

Maleic anhydride (188.2 g, 1.92 mol) was dissolved in o-dichlorobenzene (200 mL) at 200 °C. Then di-cyclopentane (131 mL, 0.97 mol) was added dropwise. The solution was heat and then reflux for 1.5 hours. After the reaction time was over, it was cooled down to room temperature, mixture of *endo* and *exo* compounds crystallized out of the solution. The crystal was filtrated and washed with large amount of hexane to completely remove yellow color. To separate *exo* conformation out of the mixture, the crystals was recrystallized multiple times with monochlorobenzene to ensure the purity. The white solid, *exo* counterpart, was filtrate and then dried under vacuum oven.

2.3.2 Synthesis of precursor (2)
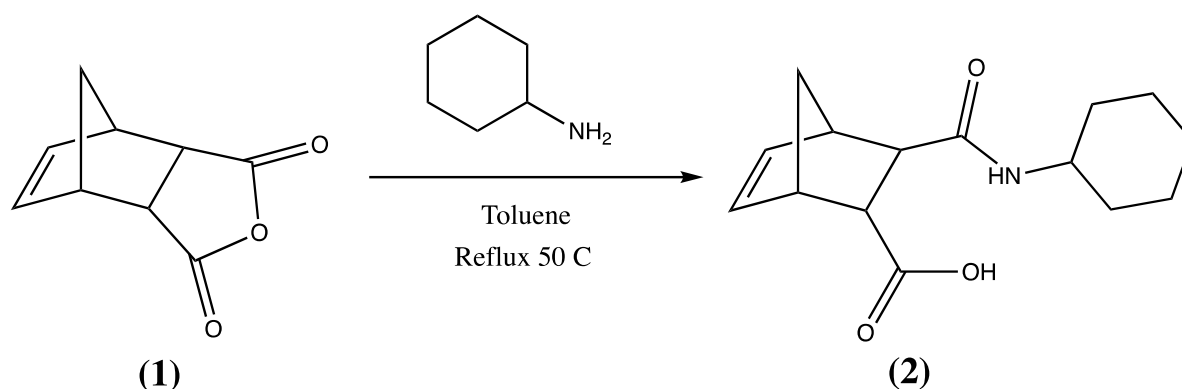
Figure 2.2 Synthetic scheme of precursor **(2)**

Precursor **(1)** (63.0 g, 0.38 mmol) was completely dissolved in 350 mL toluene under reflux condition at 50 °C. Cyclohexylamine (43.9 mL, 0.38 mmol) was then slowly added dropwise for over 30 minutes. The reaction was continued for 1 hour. After the reaction vessel was cooled down until the white solid gradually presented. The crude product of precursor **(2)** was finally filtrated and washed multiple times with toluene, following by drying in vacuum oven for overnight.

2.3.3 Synthesis of monomer M-(1)
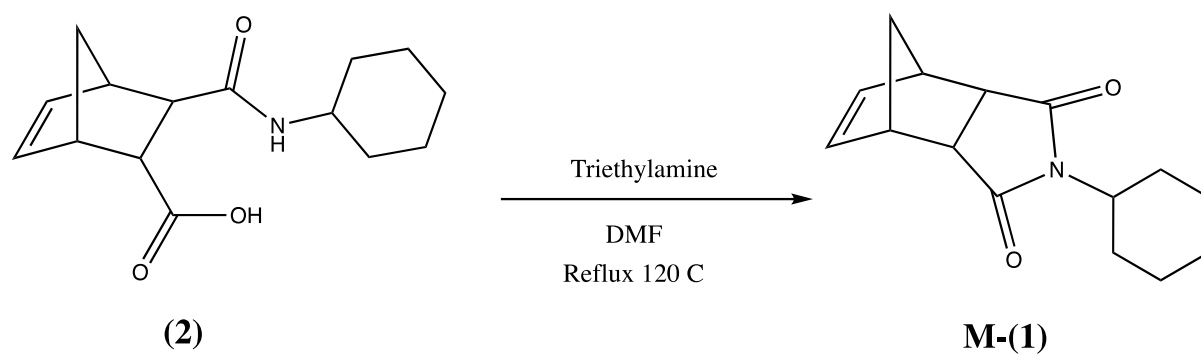
Figure 2.3 Synthetic scheme of monomer **M-(1)**

Precursor **(2)** (50.0 g, 0.189 mmol) was dissolved in 300 mL *N,N*-dimethylformamide (DMF) at 120 °C. Then the solution was added triethylamine (28.8 g, 0.283 mmol) dropwise. The reaction was refluxed for 3 hours, before cooling down to ambient temperature. The solution was precipitated in large volume of distilled water, and filtrated before drying in vacuum oven for overnight for removal of excess solvent. Crude product was recrystallized multiple times in heated methanol, following by filtration and drying under vacuum, to finally the white crystal of **M-(1)**.

2.3.4 Synthesis of precursor (3)

Figure 2.4 Synthetic scheme of precursor **(3)**

Precursor **(1)** (30.0 g, 121.8 mmol) was dissolved in 100 mL anhydrous toluene at 50 °C under inert atmosphere. Hexylamine (24.0 mL, 121.8 mmol) was then slowly added dropwise for over 30 minutes. The reaction was continued for 2 hours. After the reaction vessel was cooled down, the solution mixture was precipitated in mass amount of hexane to obtain the white solid. Precursor **(3)** was then filtrated and dried in vacuum oven for overnight.
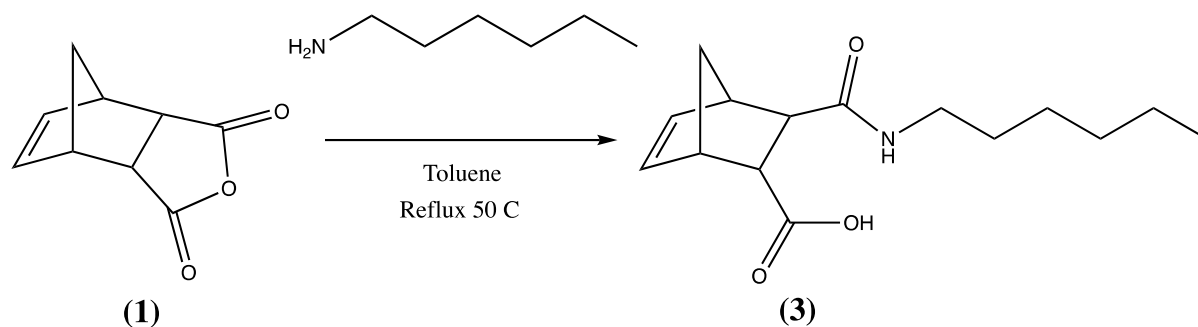
2.3.5 Synthesis of monomer M-(2)
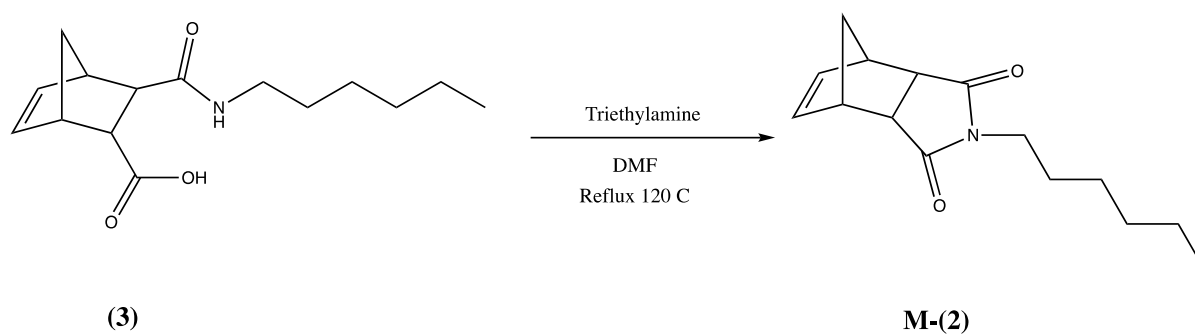
Figure 2.5 Synthetic scheme of monomer **M-(2)**

Precursor **(3)** (7.9 g, 29.7 mmol) was dissolved in 50 mL *N,N*-dimethylformamide (DMF) at 120 °C. After the mixture was completely clear, was added triethylamine (4.51 g, 44.6 mmol). The reaction was continued under reflux condition for 3 hours before cooling down to ambient temperature. The mixture was transferred to separatory funnel and washed with chloroform multiple times. The collected organic layer was then washed with brine, following by sodium sulfate (Na_2SO_4). The clear solution was evaporated to obtain brown liquid. The crude product was purified by column chromatography with solvent condition of hexane:THF = 3:2. Finally the clear yellow oil of monomer **M-(2)** was achieved.

2.3.6 Synthesis of precursor (4) – (8)
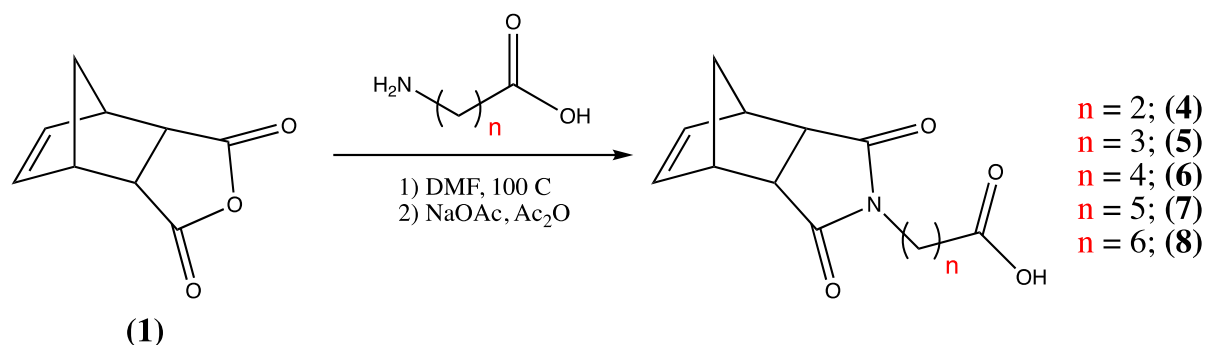
Figure 2.6 Synthetic scheme of precursor **(4)** - **(8)**

Precursor **(1)** (5.0 g, 30.45 mmol) and variety of amino acids with various carbon spacer n∗, were dissolved in 50-100 mL *N,N*-dimethylformamide (DMF) in separated vessels to obtain precursor **(4)** to **(8)**. The reaction was refluxed under inert atmosphere for 2-4 hours. After the addition of sodium acetate (NaOAc) (2.49 g, 30.45 mmol) and acetic anhydride (Ac₂O) (3.10 g, 30.45 mmol), the reaction was continued for overnight. The mixture was cooled down to room temperature before quenched with distilled water. After transfer to separatory funnel, the mixture was washed with chloroform multiple times, following by treatment with brine and Na₂SO₄. After the mixture was evaporated and dried to remove the excess solvent, the crude product was recrystallised in the mix solvent of THF and hexane. The white solid was filtrated and dried under vacuum for overnight to obtained the final product of precursor **(4)** to **(8)** with different hydrocarbon spacers.

∗; *β*-alanine (n=2), *4*-aminobutyric acid (n=3), *5*-aminovaleric acid (n=4), *6*-aminohexanoic acid (n=5), and *7*-aminoheptanoic acid (n=6)

2.3.7 Preparation of high-β phenyl vinylene thiophene vinylene bridge (FTC) chromophore
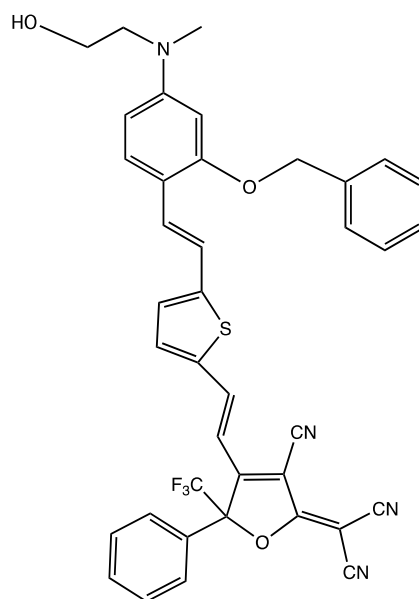
Figure 2.7 Structure of FTC chromophore used in this thesis

The FTC chromophore used for the study was originally prepared by X. Piao *et al*.[a] The maximum absorbance (λ_{max}) is at 768 nm (in CHCl$_3$). Molecular hyperpolarizability measured by hyper-Rayleigh scattering (HRS) measurement at the wavelength of 1.9 μm is 4600x10^{-30} esu. Decomposition temperature (T$_d$) of the particular EO chromophore is 210°C.

[a]X. Piao, Z. Zhang, Y. Mori, M. Koishi, A. Nakaya, S. Inoue, I. Aoki, A. Otomo, and S. Yokoyama, *"Nonlinear Optical Side-chain Polymer Postfunctionalized with High-β Chromophore Exhibiting Large Electro-optic Property", J. Polym. Sci. Part A, vol. 49, pp. 47-54, 2011*

2.3.8 Synthesis of monomer M-(3)-(7)
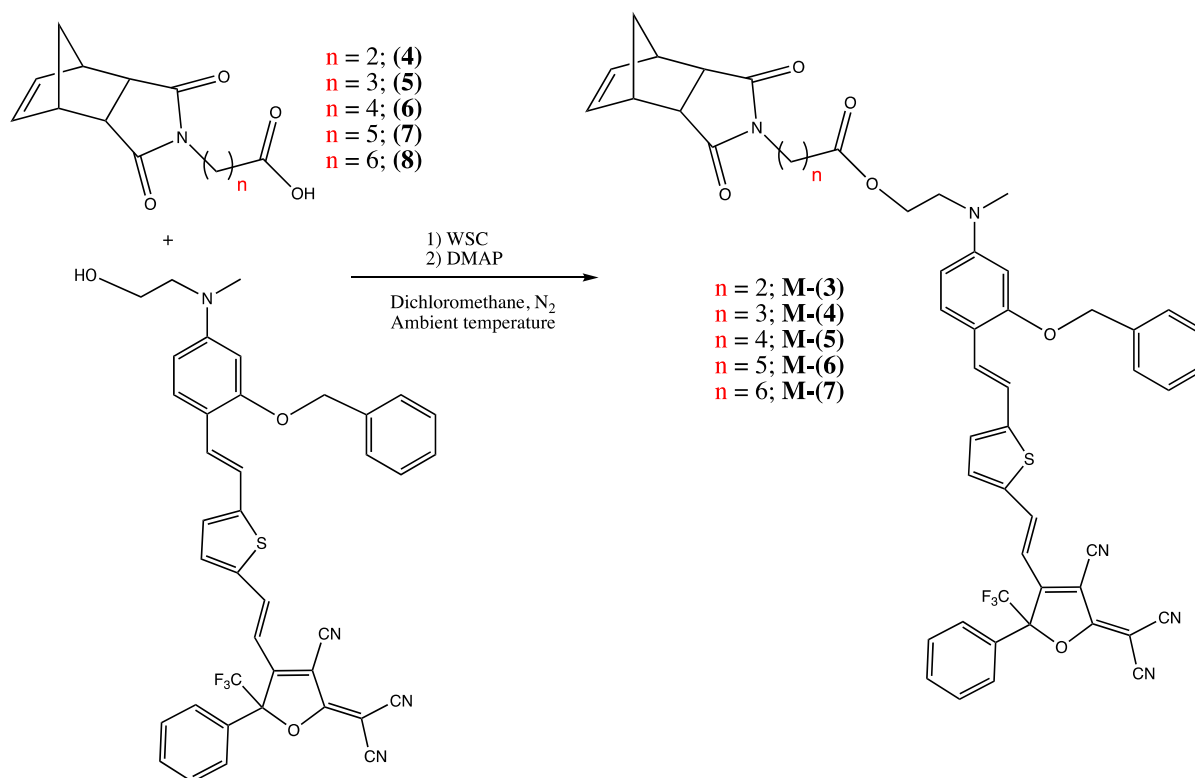
Figure 2.8 Synthetic scheme of monomer **M-(3) – (7)**

Monomers **M-(3) – (7)** were prepared by the same procedure. Precursor (4), (5), (6), (7), or (8) were transferred into three-necked flask, and flushed with nitrogen. Anhydrous dichloromethane (DCM) was then added. The reaction vessel was cooled down by ice bath, before addition of *N*-(*3*-dimethylaminoproply)-*N'*-ethylcarbodiimide hydrochloride (WSC) and *4*-dimethylaminopyridine (DMAP). The reaction was stirred to ensure complete dissolve. *Equal equivalence of the FTC chromophore* was then added into the vessel, following by removal of the ice bath to let the reaction continue at the ambient temperature for overnight. The complete reaction was confirmed by TLC, after that it quenched by distilled water. The solution mixture was transferred to separatory funnel and washed with DCM (multiple times), brine, distilled water, and Na_2SO_4, respectively. After the excess solvent was evaporated, the

purification was done by column chromatography at solvent condition of DCM:MeOH = 19:1. Finally, the dark green powder of monomer **M-(3)-(7)** were obtained after removal of excess solvent by vacuum oven.

2.3.9 Polymer synthesis by ring opening metathesis polymerisation (ROMP)

The mass of monomer **M-(1)** or **M-(2)** in each batch were constant at 1.0 g, while the mass of chromophore monomer **M-(3)** to **M-(7)** were varied depending on desired FTC chromophore loading density which were ranging from 20 to 60 wt%. The mixture powders of the monomers were charged into Schenk tube, following by stirring under vacuum and heating by heat gun to remove moisture residue. The vessel was then filled with nitrogen gas. After addition of 10-15 mL anhydrous chloroform ($CHCl_3$), the mixture was stirred for 30 minutes at ambient temperature to confirm complete dissolve. In the other small flask was added calculated mass amount of Grubbs 3_{rd} generation catalyst (G3), before drying under vacuum and flushing with nitrogen, respectively. To the small flask was injected 2 ml anhydrous $CHCl_3$. The catalyst solution was then quickly transferred to the monomer mixture in Schenk tube by syringe. The polymerisation was allowed to propagated for 24 hours under inert atmosphere for 24 hours to ensure complete conversion. After the reaction time was finished, 2 ml ethyl vinyl ether (EVE) was added as termination process. After being stirred for an hour, the solution was transferred to small round bottomed flask and evaporated the excess solvent. The crude product was re-dissolved with $CHCl_3$ and precipitated into MeOH for 1-2 times. The dark green powder was collected by filtration using Buchner funnel under vacuum. Finally, the product was dried under vacuum oven for overnight to completely remove the solvent residue.

CHAPTER III

Norbornene-dicarboximide (NDI) Based Monomers and Electro-optic (EO) Polymers

In order to achieve the requirements of organic EO polymers which are applicable for device fabrication, there are several alternatives of polymer systems utilized as EO polymers. Herein, an overview of major polymer systems, with their advantages and disadvantages is briefly discussed. The thermos-physical characterizations of synthetic monomers and EO polymers will be also taken in accounted in this chapter.

3.1 Material requirements

In general, large nonlinearities is the key element for organic EO materials for fabrication of exceptional future generation devices for telecommunications. However, there are many other essential parameters needed to be simultaneously optimized, to incorporate materials into practical devices.

First of all, EO devices are expected to be used in long term. Therefore, EO chromophore should be chemically stable high electrical voltage during poling. Moreover, EO polymer should also possess adequate thermal stability at elevated temperature during device processing. Thermally stable EO polymer can be initially accomplished by preparation of polymer possessing high glass transition temperature. This is to maintain second order nonlinearity from non-centrosymmetric order of EO chromophores for long periods of time.

Photostability is also one of the crucial parameters. EO chromophore, as well as polymer materials are necessarily to sufficiently withstand high intensity laser without molecular degradation that causing loss of nonlinearity. [1]

The other key performance of EO devices is optical loss. In general, there are several sources causing optical loss including absorption, scattering, polarization dependence, reflection, radiation, and fiber coupling. [2, 3] Absorption loss is the major loss occurring in polymeric EO materials owning to either vibrational absorption (C-H vibrational overtones) or electronic absorption (HOMO-LUMO charge transfer). Moreover, good optical transparency and solubility in spin-coating solvents are also essentially required for polymeric host and EO chromophore to prevent scattering loss. [4]

3.2 Polymer systems

3.2.1 Host-guest system

Host-guest system is polymeric nonlinear system firstly to be investigated by simple incorporation of EO chromophore as guest into polymer host. [5, 6, 7, 8] In this system, EO chromophores should be highly soluble in polymer matrix with consistent compatibility without phase separation to occur in film formation process. Moreover, selected polymer host should exhibit high T_g, since chromophore often acts as plasticizer, reducing thermal stability of the material. This causes the reduction in temporal stability of EO polymers due to orientational relaxation. [1]

3.2.2 Main chain system

In main chain system, EO chromophore are chemically incorporated into polymer backbone itself. The main purpose is to restrict poled-order relaxation, by preventing segmental rotation

of chromophores, resulting in excellent temporal stability. [9] Although there are variety of main chain EO polymers examined, this polymeric system, however, mostly shows poor processabilities (solubility and poling efficiency) in practical. Moreover, the choice of EO chromophores applicable for high loading polymerisation is also limited and difficult to achieved.

3.2.3 Cross-linked system

Cross-linked system is the other feature to accomplish high orientational stability. By lattice hardening which each polymer chain connected *via* covalent bond, the movement of poled-ordered EO chromophores is thus restricted. In general, there are two approaches to cross-link polymer chains, which are photo-induced and thermally-induced cross-linking. However, UV or visible lights applied to activate photo-induced initiator could stimulate EO chromophore degradation due to molecular absorption. [10] Hence, thermally-induced attempt has been used more widely. [11] Although this particular method could improve mechanical properties, crucial concern is insufficient poling efficiency as well as low solubility in similar to main chain system [12].

3.2.4 Side-chain system

For side-chain polymer, EO chromophore is covalently attached to polymer backbone as pendant *via* flexible spacer. [12] With this scheme, high concentration of EO chromophore can be incorporated without phase separation or crystallisation, resulting in large nonlinear response. [13] While maintaining good solubility, this system also promotes high orientational stability because of hindered movement of chromophore by its connection with polymer chain. In addition, glass transition temperature of side-chain polymer has proven to be enhanced as compared to guest-host systems. [1, 14] Side-chain EO polymers have been extensively

developed using several polymer backbones including polyimides, polycarbonates and polymethylmethacrylate (PMMA), which is the most widely used. [15, 16, 17, 18]

a)

b)

c)

d)

Polymer main chain

D-π-A   EO Chromophore
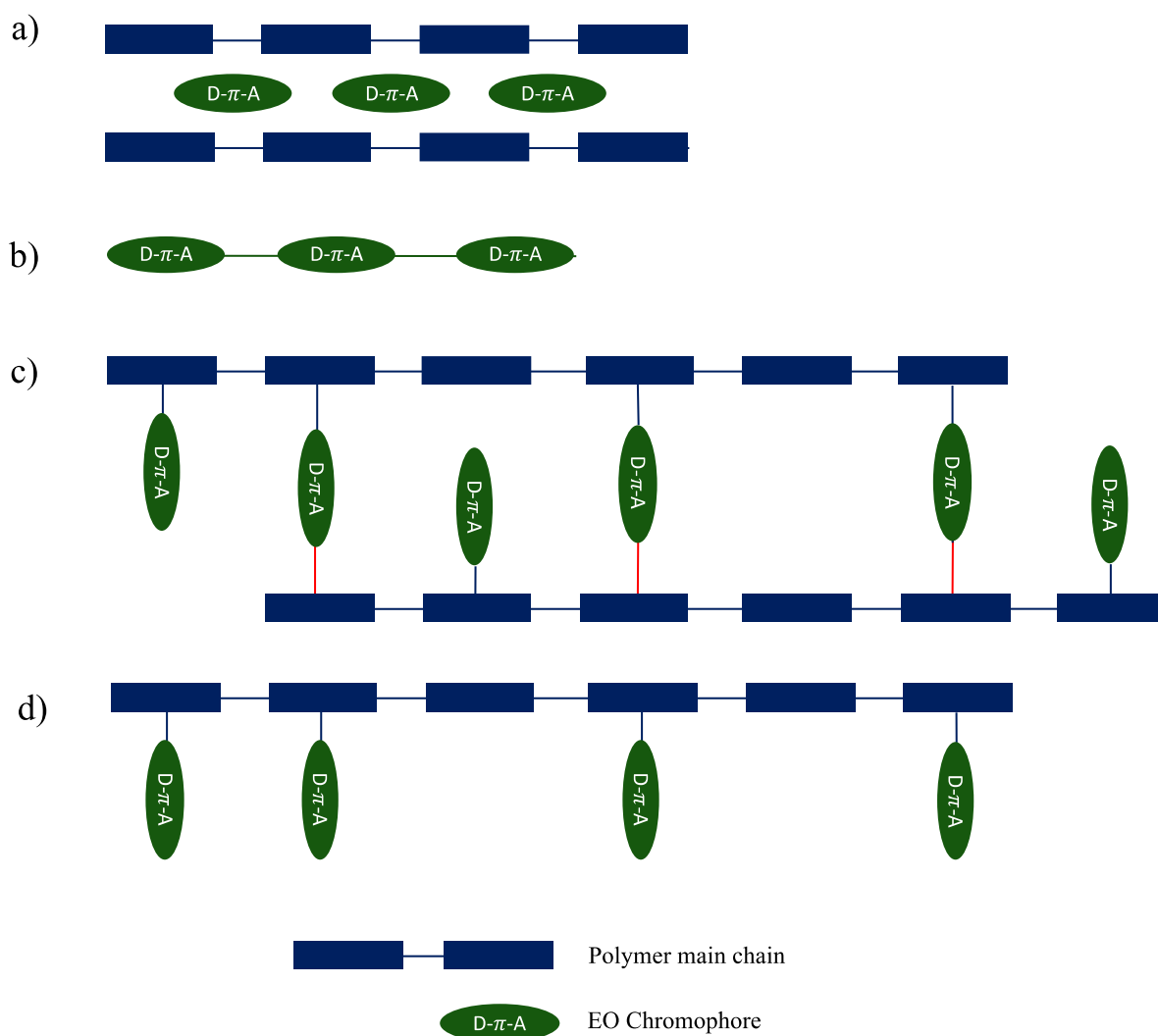
Figure 3.1 Illustration of EO polymer systems;

a) Guest-host, b) Main chain, c) Cross-linked, and d) Side-chain

3.3 Norbornene-dicarboximide (NDI) based monomers

As mentioned in section 3.2, each polymer system has pros con cons. However, in this work, we aimed to produce highly thermal stable EO polymers. Therefore, we selected to focus on the synthesis of side-chain EO polymers.

Potential polymers to be utilized as EO polymers, have to show high temperature resistance. This is to maintain the stability of asymmetric alignment of EO chromophore while processing at elevated temperature. Poly(methyl methacrylate) or PMMA has been widely used the most due to its transparency, and low cost. Moreover, by adjusting its substituents, glass transition temperature (T_g) can be substantially varied ranging from 85°C to 165°C. However, production of amorphous PMMA, radical polymerisation is generally performed. The radical initiators, such as azobisisobutyronitrile (AIBN), usually cause the degradation of electron-rich compound like EO chromophore. Hence, the synthesis of side-chain EO polymer are exhibited by post-polymerisation procedure as follows;

1) Radical polymerisation of PMMA backbone

2) Grafting of EO chromophore onto PMMA

3) Dialysis; removal of unreacted EO chromophore by large amount of solvent

which often resulted in long preparation time and low yield of EO polymers. Since our goal in not only to provide highly thermal stable EO polymer, but also to simplify preparation of EO polymers, in order to apply particular EO polymers to industrial level.

The promising polymer we have selected to study in this thesis was polynorbornene-dicarboximide (poly(NDI)s). Poly(NDI) were reported by *Jawed Asrar* since 1992 as highly thermal stable thermoplastic polymers. [19] NDI monomers, containing cyclic olefins, can be polymerised *via* ring opening metathesis polymerisation (ROMP) due to its ring strain (see

Figure 3.2). This enables the production of polymers to be carried out in bulk without any major byproducts. Moreover, metathesis polymerisation is considered to be a versatile reaction, that can be driven to complete conversion of monomers. This would be hugely advantageous for industrial production to obtain the finished polymers in one step without further use of solvent in large amount for purification.
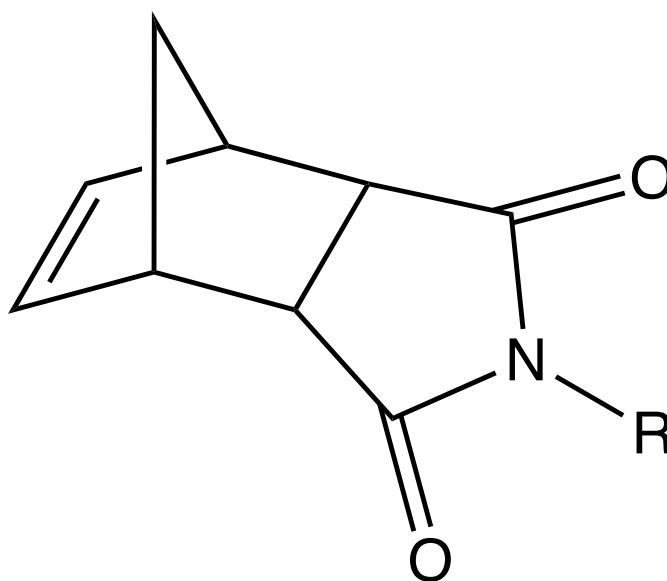
Figure 3.2 General schematic illustration of Norbornene-dicarboximide (NDI)

In addition, the release of high ring strain during polymerisation of norbornene makes free energy of the reaction highly negative, leading to great tolerance toward variety of polar substituted functionalities. [20] This has also led to synthesis of wide range of interesting copolymers since numbers of catalysts can be used as initiators in metathesis polymerisation.

3.4 Characterizations of NDI monomers

In this thesis, all NDI monomers were prepared and characterized by 1H NMR and mass spectroscopy. NDI monomer **M-(1)** with cyclohexyl and **M-(2)** with hexyl were prepared in order to optimize thermal stability of EO polymers. As seen in **Fig 3.3**, the singlet peak at 6.28

ppm integrating 2 protons has been assigned to alkenic protons labelled as **a** in both monomers, which is the polymerisable site for ROMP. Precursor (1), which is the starting material for preparation of these two NDI monomers were prepared to be in *exo* isomer by multiple recrystallisation in *o*-chlorobenzene. This is because it is well known that *exo* NDI is found to be polymerised into polymer with high conversion easier than that of *endo* isomer, due to steric hindrance. [19] Mass spectroscopy in ion mode FAB+ was also used to confirmed m/z of **M-(1)** ($C_{15}H_{19}NO_2$, 245.14) and **M-(2)** ($C_{15}H_{21}NO_2$, 247.16) as 246.3201 and 248.1301, respectively. The use of different side groups, cyclohexyl and hexyl, were aimed to study the mobility of polymer coins, in which affects to thermal stability, as well as molecular weight distribution of polymer system.
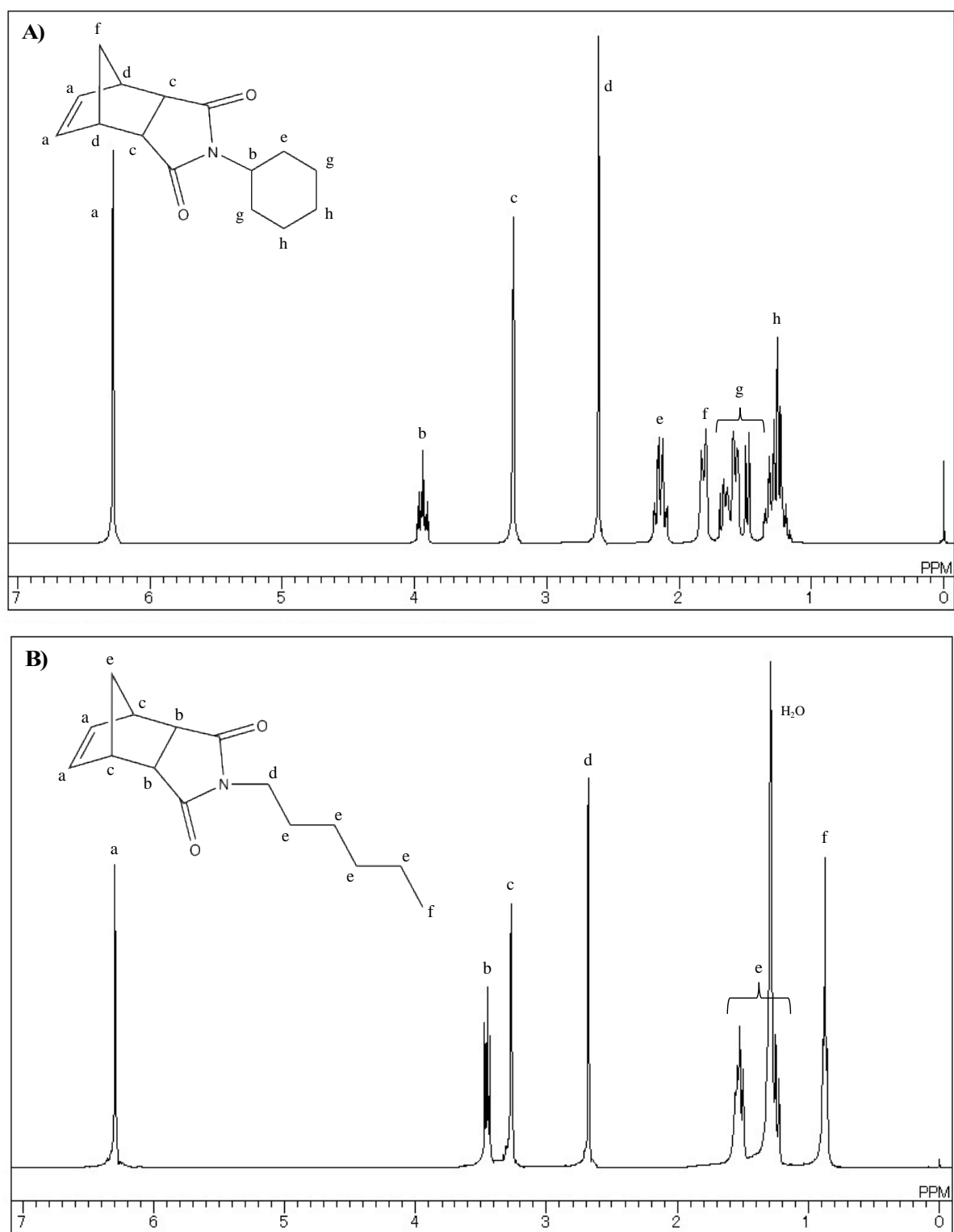
Figure 3.3 ^{1}H NMR spectra of monomer A) **M-(1)** and B) **M-(2)**

Figure 3.4 consists of ₁H NMR spectra of Cr-NDI monomers **M-(3)**, **(4)**, **(5)**, **(6)** and **(7)**, in which chemical shifts were assigned to individual protons. Furthermore, high resolution mass spectroscopy was also measured to confirmed the structure of chromophore NDI monomers. The results showed the calculated mass of all monomers exactly matched with measured values. as follows;

M-(3); ₁H NMR (400 MHz, CDCl₃) δ: 7.79 (1H, d), 7.49-7.14 (15H, m), 6.58 (1H, d), 6.34 (1H, d), 6.25 (3H, d), 5.20 (2H, s), 4.21 (2H, t), 3.75 (2H, t), 3.61 (2H, t), 3.25 (2H, s), 3.02 (3H, s), 2.66 (2H, s), 2.56 (2H, t), 1.48 (1H, d), 1.22 (1H, d) ppm.

 m/z (FAB+); 907.2650 ($C_{51}H_{40}F_3N_5O_6S$, 907.27)

M-(4); ₁H NMR (400 MHz, CDCl₃) δ: 7.80 (1H, d), 7.63-7.14 (15H, m), 6.92 (1H, d), 6.58 (1H, d), 6.26 (2H, d), 5.21 (2H, s), 4.23 (2H, t), 3.62 (2H, t), 3.49 (2H, t), 3.23 (2H, s), 3.03 (3H, s), 2.66 (2H, s), 2.27 (2H, t), 1.84 (2H, m), 1.48 (1H, d), 1.16 (1H, d) ppm.

 m/z (FAB+); 921.2810 ($C_{52}H_{42}F_3N_5O_6S$, 921.28)

M-(5); ₁H NMR (400 MHz, CDCl₃) δ: 7.78 (1H, d), 7.61-6.91 (15H, m), 6.57 (1H, d), 6.33 (1H, d), 6.26 (3H, d), 5.20 (2H, s), 4.21 (2H, t), 3.60 (2H, t), 3.44 (2H, t), 3.25 (2H, s), 3.01 (3H, s), 2.63 (2H, s), 2.28 (2H, t), 1.48 (1H, d), 1.58 (3H, m), 1.48 (1H, d), 1.19 (1H, d) ppm.

 m/z (FAB+); 935.2965 ($C_{53}H_{44}F_3N_5O_6S$, 935.30)

M-(6); ₁H NMR (400 MHz, CDCl₃) δ: 7.80 (1H, d), 7.63-7.16 (15H, m), 6.94 (1H, d), 6.55 (1H, d), 6.35 (1H, d), 6.27 (2H, s), 5.20 (2H, s), 4.21 (2H, t), 3.62 (2H, t), 3.43 (2H, t), 3.23 (2H, s), 3.02 (3H, s), 2.65 (2H, s), 2.23 (2H, t), 1.63-1.18 (8H, m) ppm.

 m/z (FAB+); 949.3122 ($C_{54}H_{46}F_3N_5O_6S$, 949.31)

M-(7); 1H NMR (400 MHz, CDCl3) δ: 7.790 (1H, d), 7.63-7.15 (15H, m), 6.93 (1H, d), 6.57 (1H, d), 6.35 (1H, d), 6.27 (2H, s), 5.19 (2H, s), 4.21 (2H, t), 3.60 (2H, t), 3.42 (2H, t), 3.26 (2H, s), 3.02 (3H, s), 2.65 (2H, s), 2.24 (2H, t), 1.60-1.17 (10H, m)

m/z (FAB+); 963.3277 ($C_{55}H_{48}F_3N_5O_6S$, 963.33)
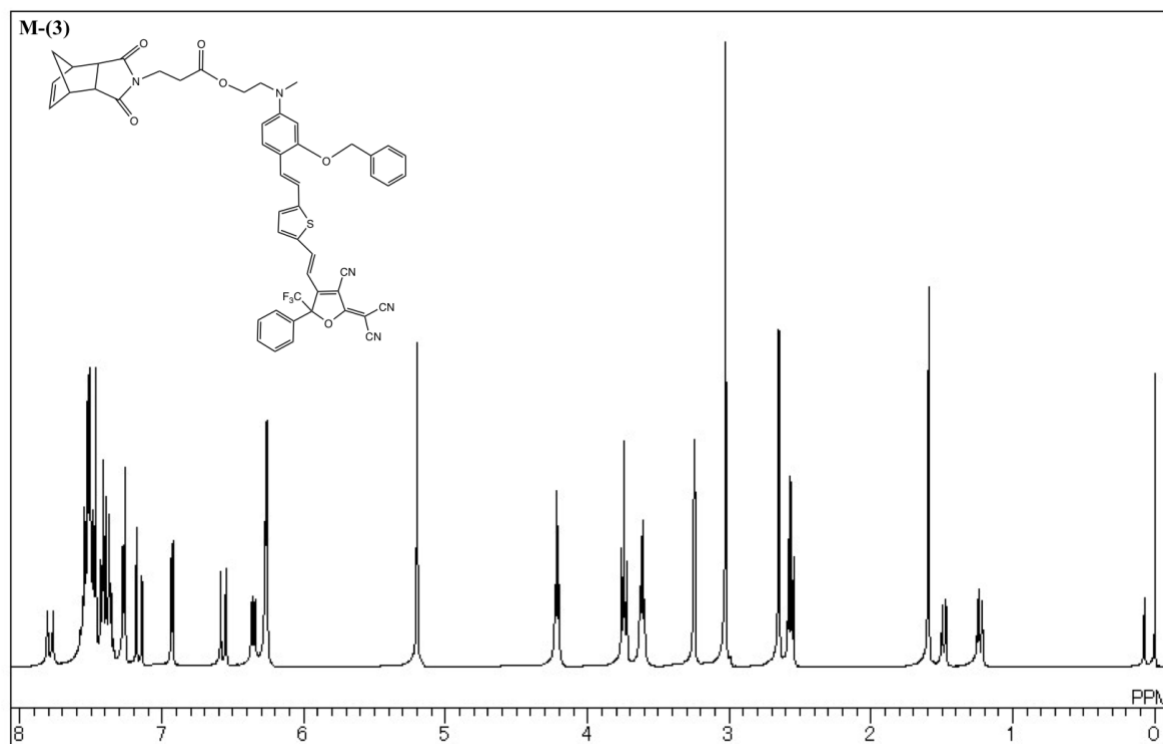
Figure 3.4 1H NMR spectra of monomer **M-(3), (4), (5), (6)** and **M-(7)**
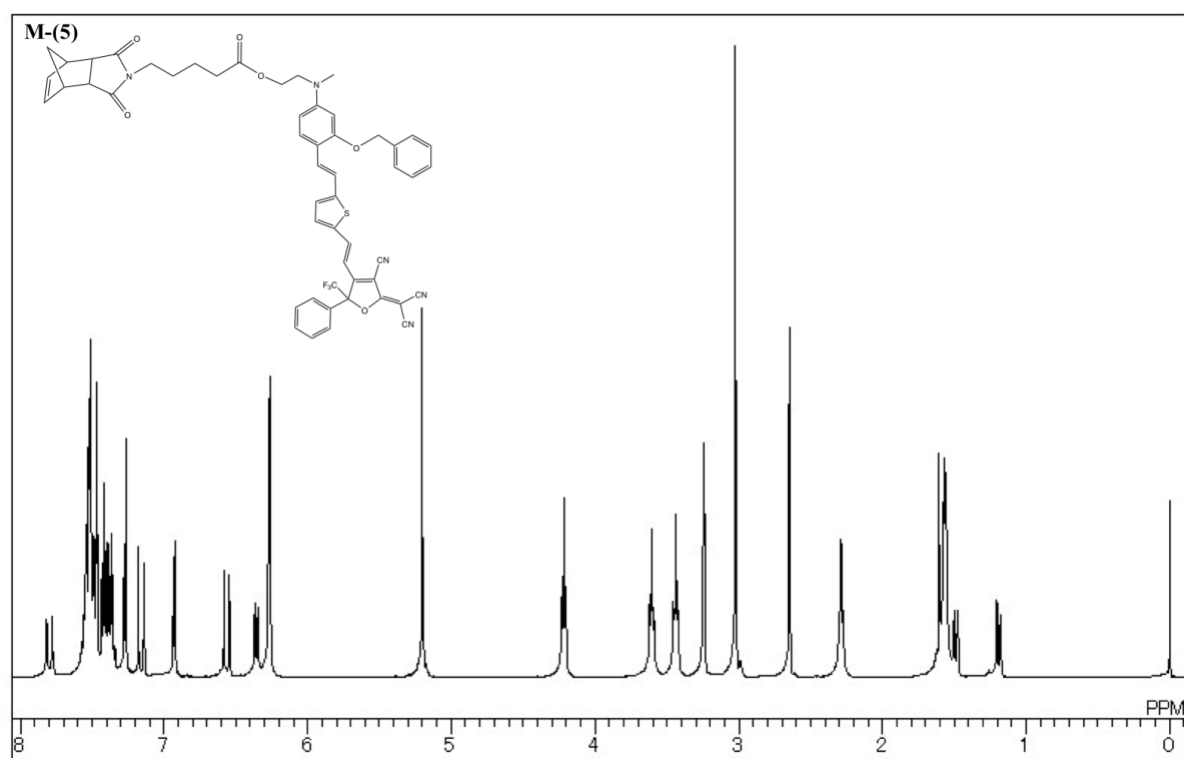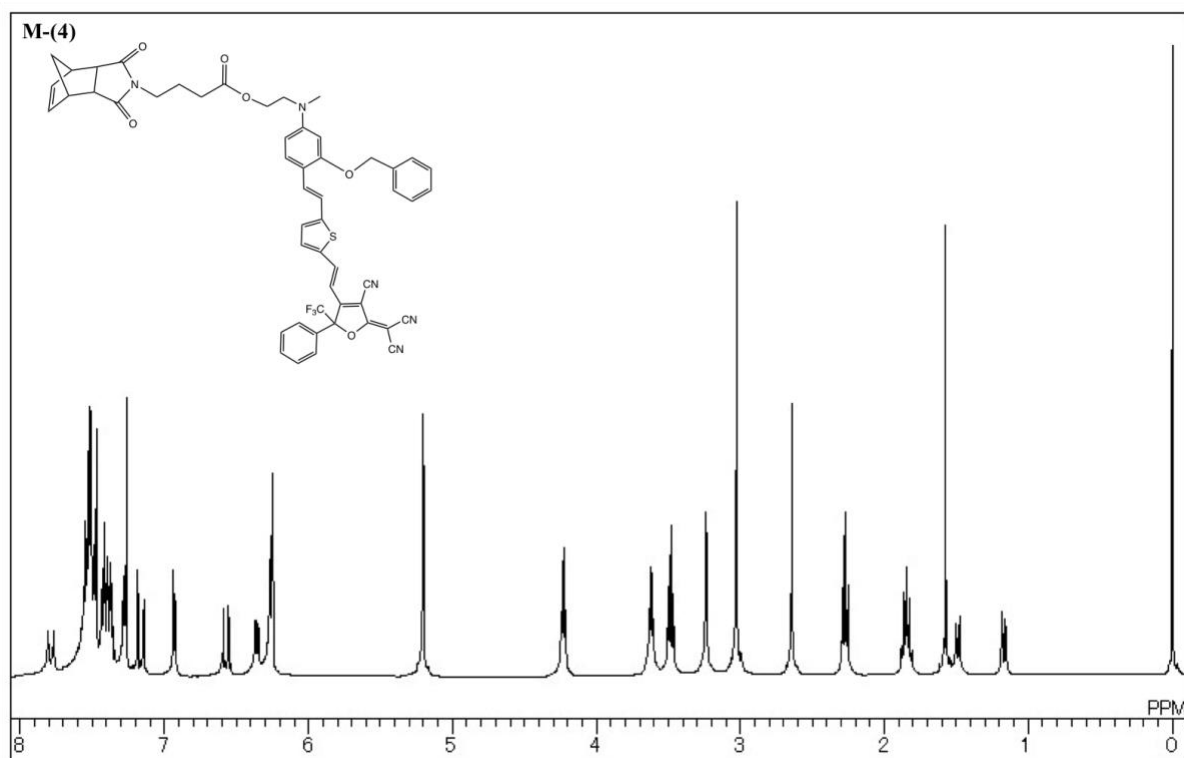
Figure 3.4 1H NMR spectra of monomer **M-(3), (4), (5), (6)** and **M-(7)** (continue)
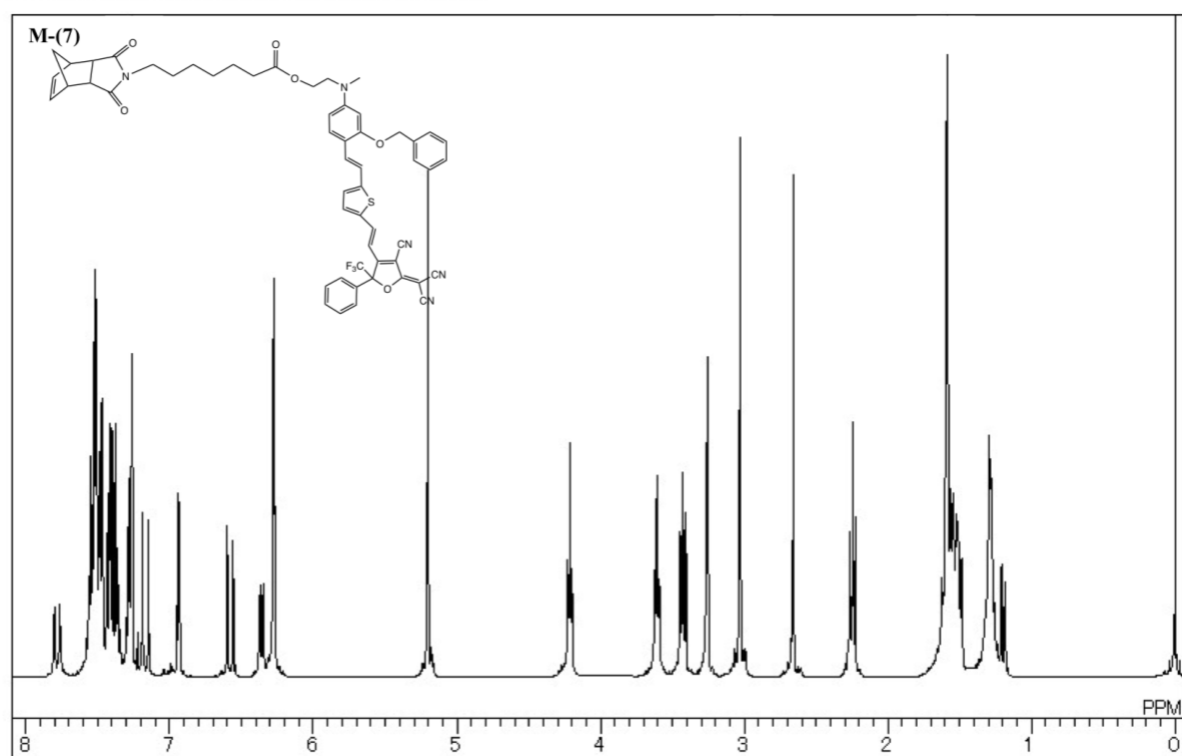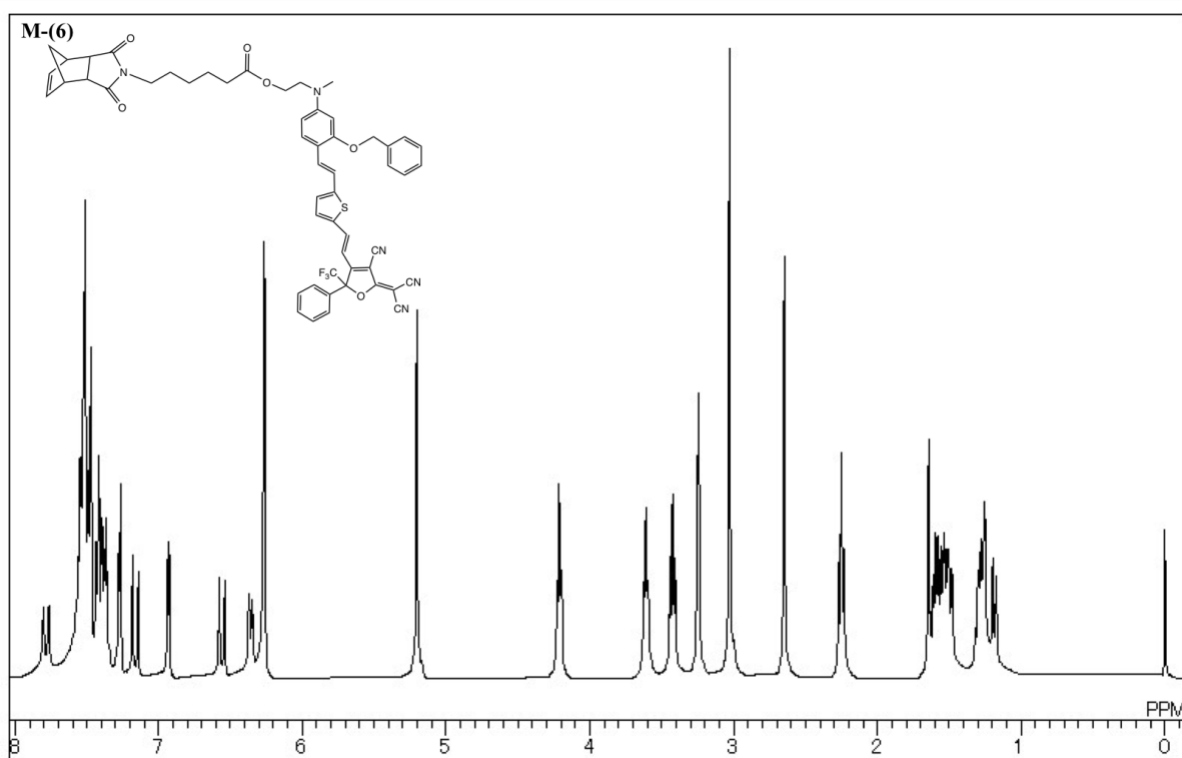
Figure 3.4 ${}_1$H NMR spectra of monomer **M-(3), (4), (5), (6)** and **M-(7)** (continue)
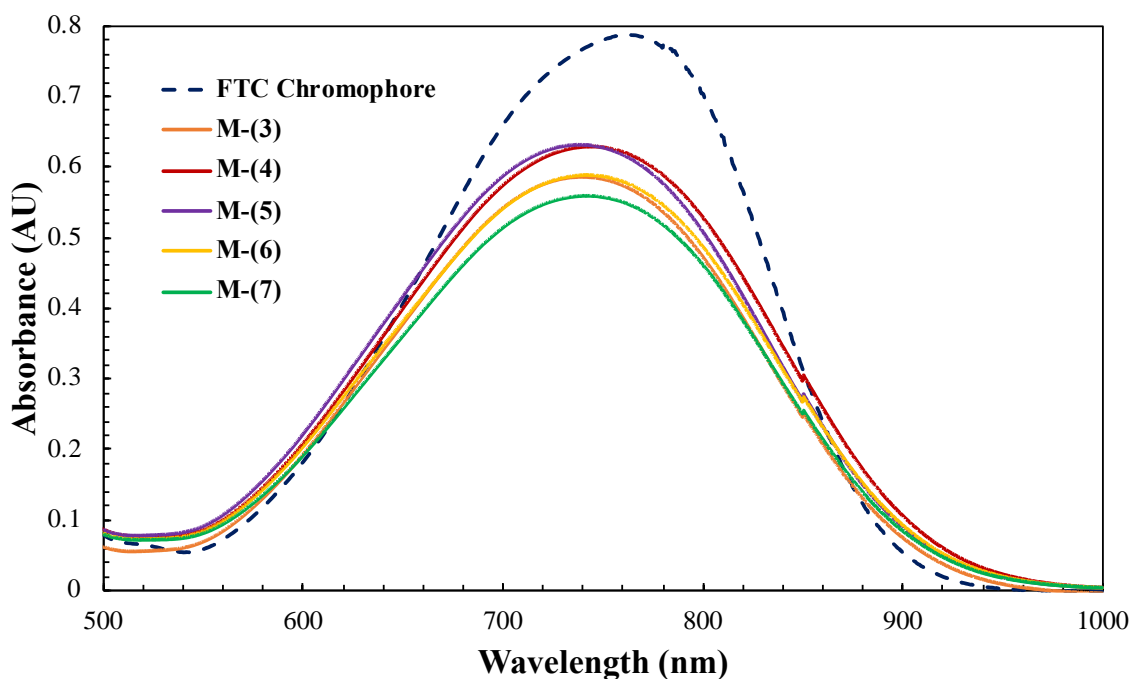
Figure 3.5 UV-Vis spectra of FTC chromophore (Cr) and Cr-NDI monomers

UV spectra of **M-(3)** to **M-(7)** in THF were displayed in **Figure 3.5**. In comparison to single FTC chromophore, maximum absorbance (λ_{max}) of Cr-NDI monomers slightly blue shifted to shorter wavelength due to the addition of NDI moiety. Each monomer was calculated to confirm the consisting of 76, 75, 73, 72 and 71 wt% of FTC chromophore, respectively.

3.5 Ring opening metathesis polymerisation (ROMP) using Grubbs 3$_{rd}$ generation catalyst

As mentioned that all EO polymers studied in this thesis will be prepared *via* ring opening metathesis polymerisation (ROMP) using Grubbs 3$_{rd}$ generation catalyst as an initiator, which considered as mild reaction for EO chromophore.
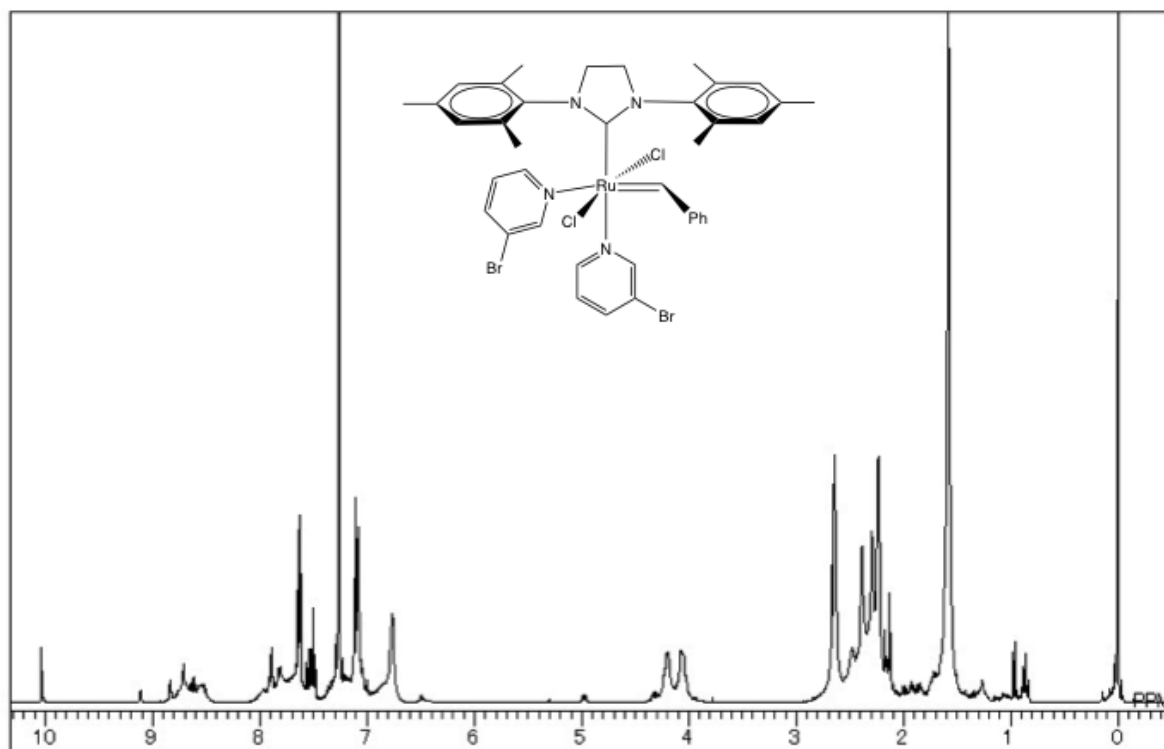
Figure 3.6 1H NMR spectrum of Grubbs 3rd generation catalyst (G3), an initiator for ROMP

The development of Grubbs catalyst, ruthenium-based metathesis catalyst, was to achieve the goal of preparation interesting polymeric structures without limitation of poor functional-group tolerance due to the oxophilicity of the metal center. Moreover, the other major advantage is the simple handling of the ruthenium catalyst without the use of a glovebox, since the catalyst shows amazing tolerance to oxygen and aqueous media. [21] Since then, the development of Grubbs catalyst has been intensively improved, leading to broad potential for syntheses of novel macromolecules, especially G3. [22, 23, 24, 25, 26]
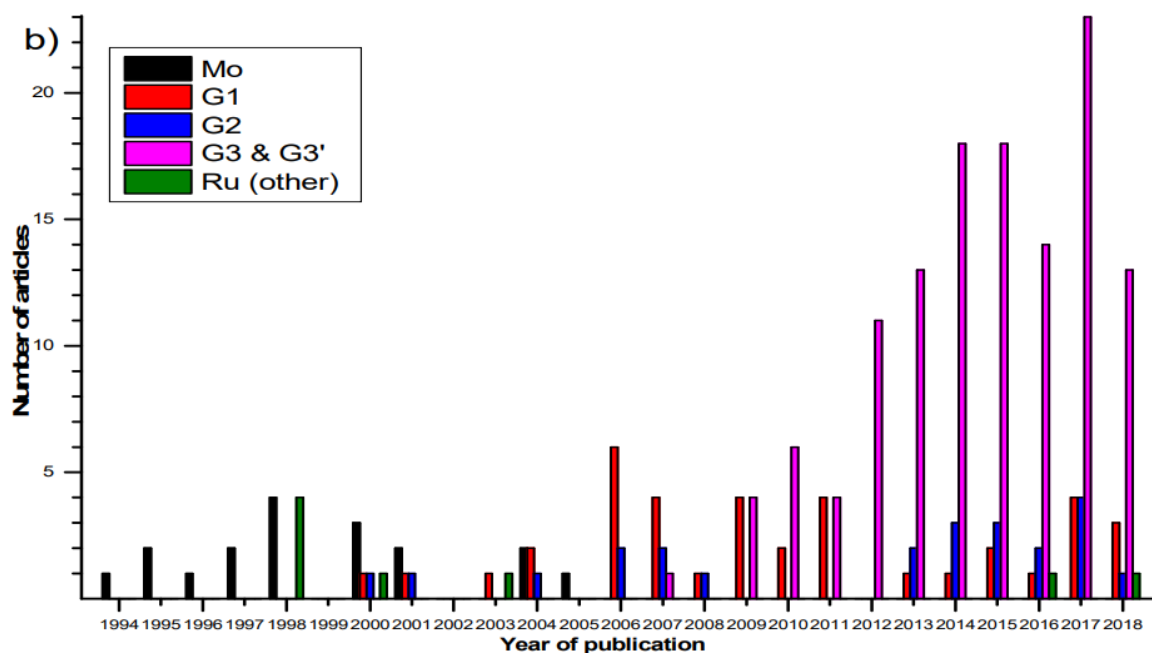
Figure 3.7 Number of articles published per year, where each catalyst is mentioned [27]
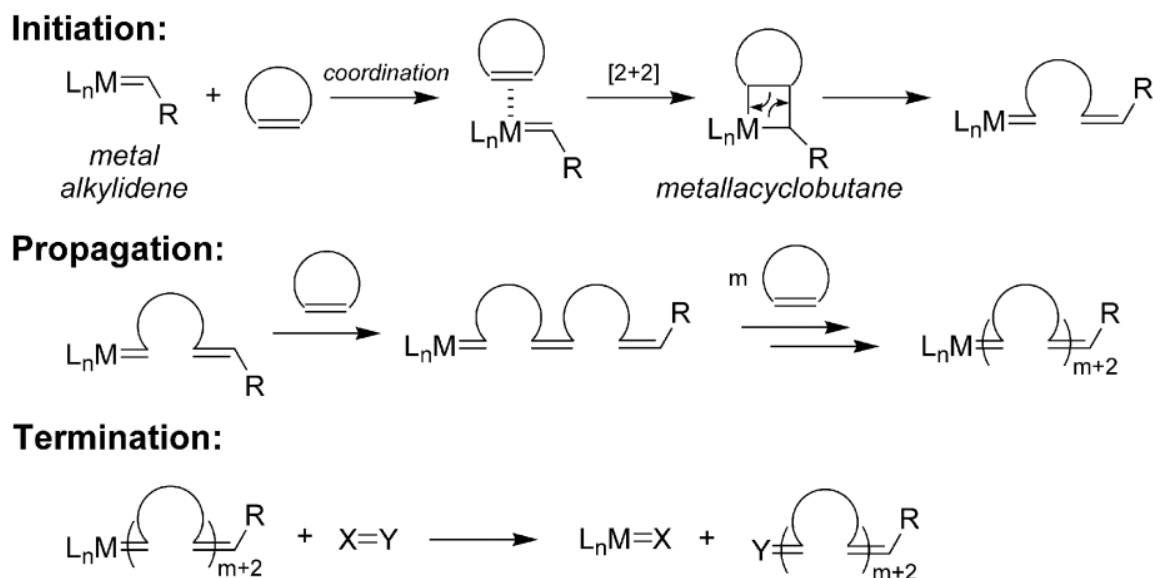
Figure 3.8 General mechanism of ROMP reaction of cyclic olefins [27]

Figure 3.8 shows the proposed mechanism of ROMP reaction of cyclic olefins proposed by

Yves Chauvin. The initiation step is started by the coordination of metal alkylidene complex

to cyclic olefin by *[2+2]* cycloaddition, forming a metallacyclobutane intermediate. The

activated intermediate then propagates to other cyclic olefins to achieve polymer chain. The propagation is generally terminated by vinylic reagent, which reacts with metal carbine of propagating polymer end and remove the metal from the chain.

3.6 Characterization of EO homopolymers and their glass transition temperatures

The characterization of homopolymers which were not consisted of EO chromophore monomer is to understand characteristics NDI based polymers and their thermal property. **Figure 3.9** shows NMR spectra of poly(cyclohexyl-NDI) in a) and poly(hexyl-NDI) in b). The polymerisation could be confirmed by broader spectra, in comparison to single monomers. In addition, $_1$H chemical shift at 5.61 and 5.55, which refer to vinylene group in *trans* and *cis* conformations, respectively, could also assure the opened ring due to ROMP as well.

The two homopolymers, showed huge difference in their T_g as seen in **Table 3.1**. While **H-(1)** exhibited high T_g at 210°C, **H-(2)** displayed much lower T_g at 76°C. This is due to more flexibility in hexyl chain compared to cyclic pendant, which required lower much temperature for phase change. Therefore, we selected to use these two monomers, as thermal control units for the evaluation of well-balanced EO polymer possessing excellent and stable EO coefficient at elevated temperature in this thesis.

Polymer	Side-group	T_g (°C)
H-(1)	Cyclohexyl	210
H-(2)	Hexyl	76

Table 3.1 Glass transition temperature of homopolymer **H-(1)** and **H-(2)**
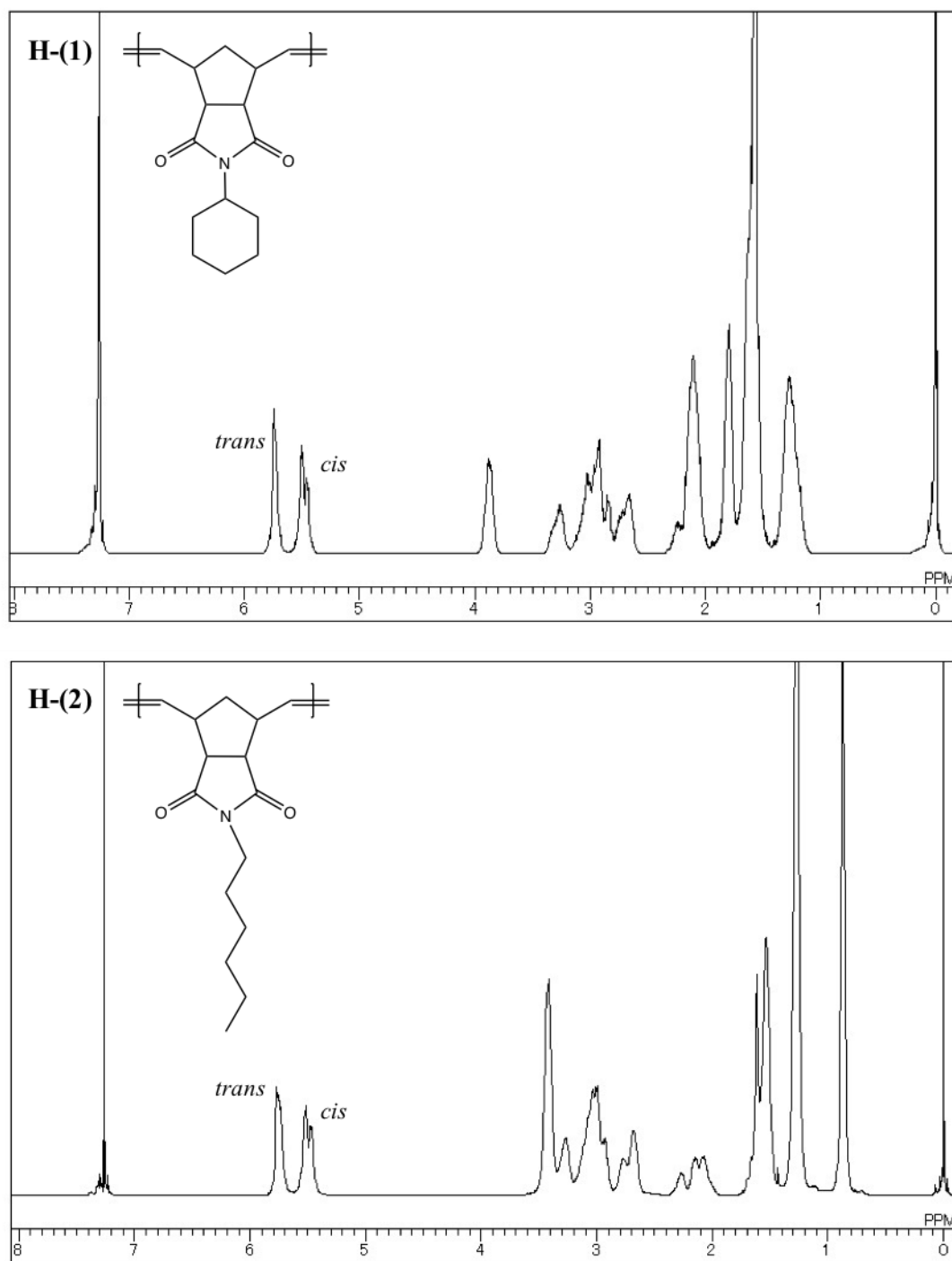
Figure 3.9 1H NMR spectra of two homopolymers poly(cyclohexyl-NDI) **H-(1)** and

poly(hexyl-NDI) **H-(2)**

3.7 Characterizations of EO copolymers

EO polymers studied in this thesis are copolymers in which consist of the combination between thermal control monomers, **M-(1)** or **M-(2)** and chromophore monomers **M-(3)**, **(4)**, **(5)**, **(6)**, or **M-(7)** to achieve high quality EO polymeric material for EO modulator.

3.7.1 The effect of EO chromophore loading density on thermal physical properties of EO polymers

According to **Eq.** (1-19) in Chapter I, it is suggested that concentration of EO chromophore is one of the crucial parameters to enhance EO coefficient. However, the appropriate amount of loading chromophore is necessarily to be investigated to maintain well processability of EO polymers. This section, we studied the relationship between different amount of chromophore incorporated in NDI polymers (see **Figure 3.10** and **3.11**) and their thermos-physical properties using monomers **M-(1)** and **M-(3)** as summarised in **Table 3.2**.
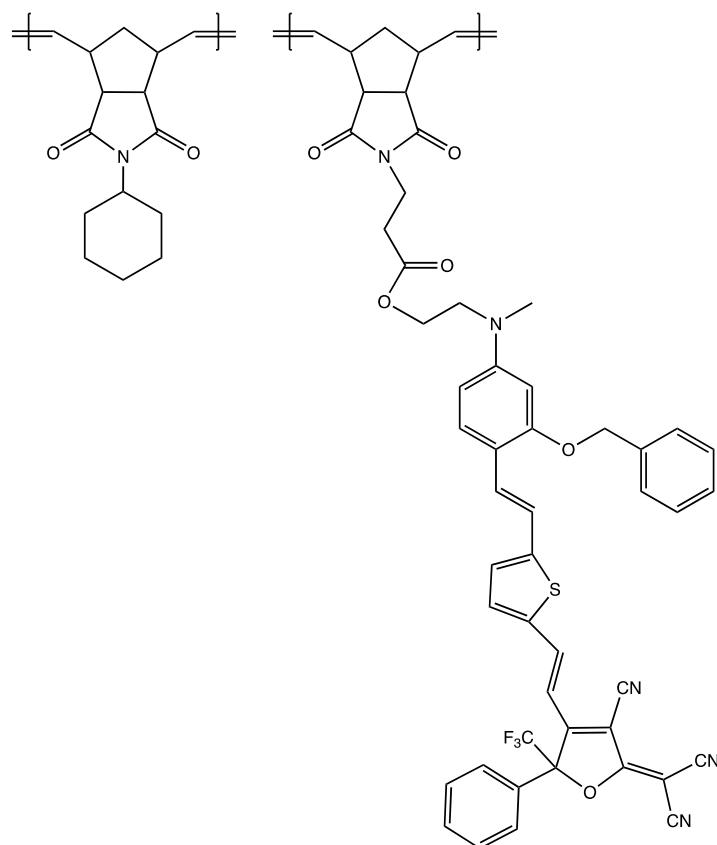
Figure 3.10 Copolymer **P-(1)** to **P-(4)** with different EO chromophore loading density
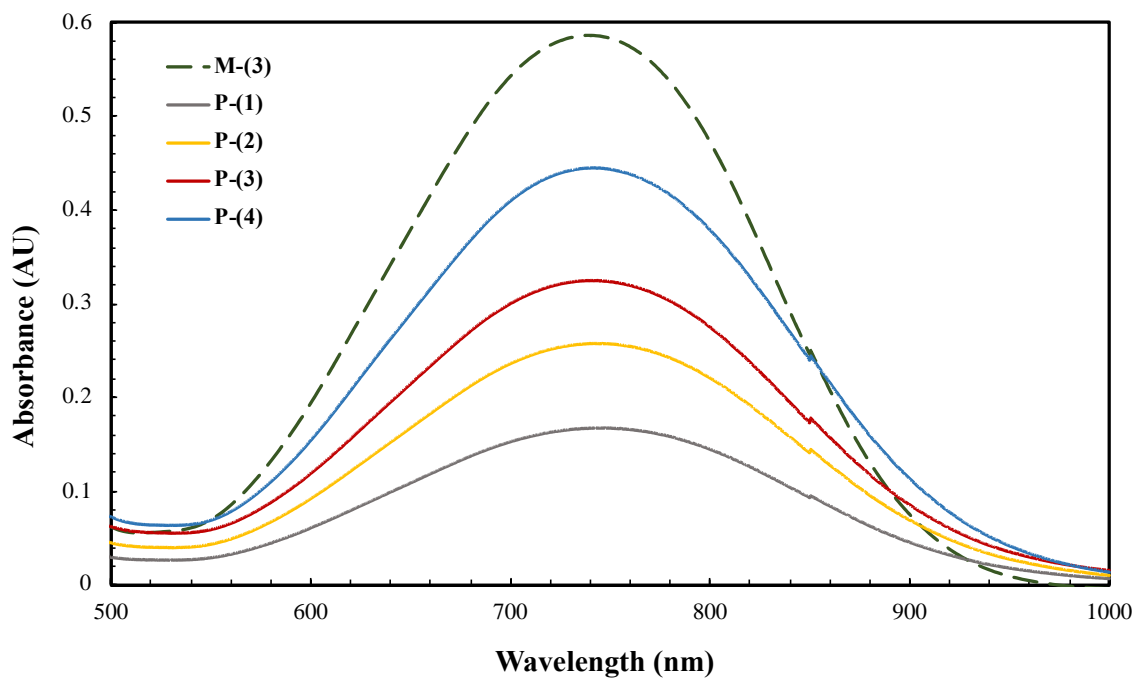
Figure 3.11 UV-Vis spectra of polymers **P-(1)** to **P-(4)** in comparison to monomer **M-(3)**

Polymer	Cr (wt%)	M_w (g/mol)	M_n (g/mol)	PDI (M_w/M_n)	T_g (°C)	%yield
P-(1)	22	18100	15200	1.19	219	89
P-(2)	34	35300	23900	1.47	193	82
P-(3)	42	43800	30200	1.44	N/A	71
P-(4)	57	74000	36800	2.00	N/A	93

Table 3.2 Physical and thermal properties of copolymers **P-(1)** to **P-(4)**

As shown in **Figure 3.11**, the amount of EO chromophore loading content was varied ranging from 21 wt% to almost 60 wt%. The loading density was quantitatively confirmed by UV-Vis absorbance spectroscopy of each EO polymer solution in THF at fixed concentration (5 mg/100 ml) in comparison with the identical concentration of **M-(3)**. The increased chromophore loading density was coherent with the higher in molecular weights and broader polydispersity index (PDI), although ROMP is well known for well-controlled polymerisation manner. This is attributed to the fact that the greater number of bulky monomer **M-(3)**, the less narrow of molecular weight distribution could be obtained as a result of less well-controlled behavior during reaction. However, polydispersity remains below 2.0 which is applicable, considering it is copolymeric system.

The major problematic difficulty in high molecular weight polymer is apparently processability towards general organic solvents. Since all these polymers consisted of π-electron-rich EO chromophore, intermolecular interaction would possibly cause partial gelation during polymerisation, which resulted in poor solubility of the final polymer product.

As explained before that NDI based polymer usually gives high thermal polymers over 200 °C. [19] However, with highly steric side group used in our study, EO chromophore, this would expectedly reduce T_g of polymers. This is because the huge chromophore pendant can act as

plasticizer reducing T_g. [28] Plus, the broader molecular weight distribution (PDI), polymers became less monodisperse, resulted in lower T_g as well. The higher chromophore loading density could also lead to the difficulty to observe their actual thermal properties. As shown in **Table 3.2**, T_g of **P-(3)** and **P-(4)** could not be clearly detected. Although the reason is not clear, it could possibly be attributed to their long polymer coils (high molecular weight) which had much stronger intermolecular and intramolecular interactions, preventing the change in mobility of bulk polymer as the heat flow in DSC risen up.

3.7.2 The Effect of flexible hydrocarbon spacer between NDI backbone and EO chromophore on thermal property of EO polymers

To investigate more on the intermolecular and intramolecular interactions which heavily impact on T_g of polymers, we performed ROMP to produce EO copolymers using different Cr-NDI monomers. While the use of **M-(1)** is fixed, length of hydrocarbon spacer was increased to C4 (**M-(5)**) and C6 (**M-(7)**) (see **Figure 3.12**).

Since the hydrocarbon chain can act as plasticizer to increase mobility of polymer coils in bulk, it is thus aimed to reduce phase change temperature of EO polymers. **Table 3.3** shows thermophysical property of NDI polymers with extended hydrocarbon linkage between NDI backbone and EO chromophore pendant, **P-(5)** (n=4), and **P-(6)** (n=6), in comparison with **P-(1)** which n=2. Although T_g remained higher than 200°C, it could be confirmed that the reduction in T_g of **P-(5)** and **P-(6)** by lengthening hydrocarbon spacer could be attributed to less intermolecular and intramolecular interactions in bulk polymer system.
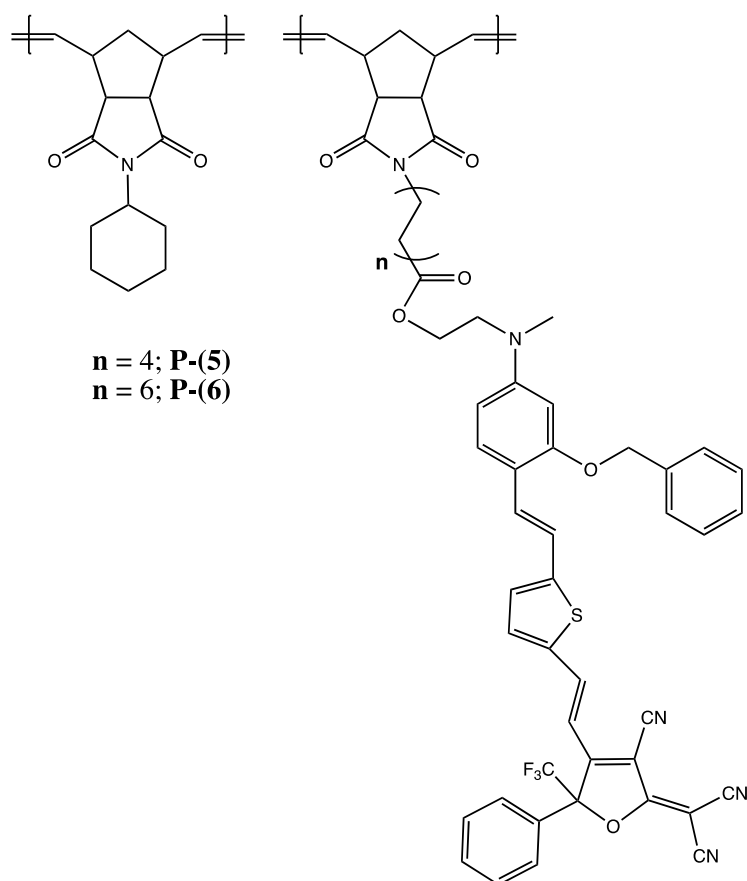
Figure 3.12 Copolymer **P-(5)** and **P-(6)** with different length of hydrocarbon spacer (n)

Polymer	n	Cr (wt%)	Mw (g/mol)	Mn (g/mol)	PDI (Mw/Mn)	Tg (°C)	%yield
P-(1)	2	22	18100	15200	1.19	219	89
P-(5)	4	21	20700	16100	1.28	216	85
P-(6)	6	24	20900	16600	1.26	210	94

Table 3.3 Physical and thermal properties of copolymers **P-(1)**, **P-(5)** and **P-(6)**

3.7.3 Optimization of thermal stability of EO polymers using hydrocarbon spacer approach

As further optimization on thermal stability of EO polymers, we polymerised copolymers using **M-(2)** as thermal control unit (**Figure 3.13**). This particular monomer has aliphatic

hydrocarbon as its side group. It was expected to significantly increase mobility of polymer

bulk, which in turn, would resulted in lower T_g.
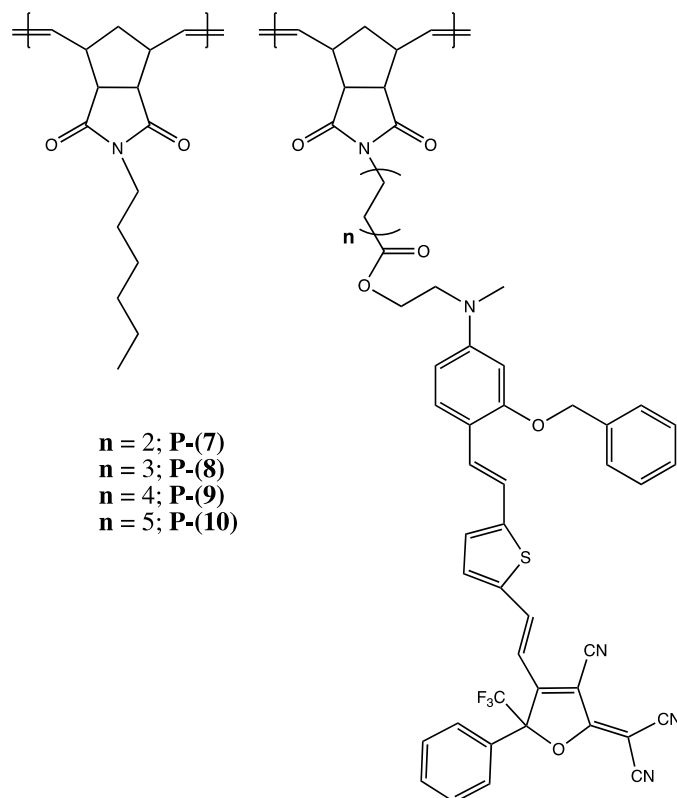
Figure 3.13 Copolymer **P-(7)** to **P-(10)** using **M-(2)** with hexyl side group and Cr-NDI

monomers **M-(3), (4), (5)**, and **(6)**

Polymer	n	Cr (wt%)	Mw (g/mol)	Mn (g/mol)	PDI (Mw/Mn)	Tg (°C)	%yield
P-(7)	2	24	41700	22300	1.87	151	79
P-(8)	3	32	35100	22600	1.55	155	89
P-(9)	4	26	43400	24900	1.74	160	76
P-(10)	5	35	35000	22500	1.54	157	94

Table 3.4 Physical and thermal properties of copolymers **P-(7)** to **P-(10)**

According to thermos-physical properties exhibited in **Table 3.4**, polymer **P-(7)** shown lower

T_g in comparison to **P-(1)**, while using same Cr-NDI monomer **M-(3)**. This could coherently

be contributed to plasticizing ability of hexyl pendant as thermal control unit, which allow more mobility of polymer chains. However, T_g remained over 200°C which is over decomposition temperature (T_d) of FTC chromophore (210°C). [29]

We then further attempted to reduce T_g by utilizing Cr-NDI monomers with longer hydrocarbon spacers, **P-(8)** – **P-(10)**. As a result, T_g dramatically declined. This confirmed that extended aliphatic spacer in between NDI backbone and EO chromophore, could controllably adjust thermal property of EO polymers.

3.8 Summary

This chapter discussed thermal-physical characterizations of NDI monomers as well as EO polymers by NMR, UV-Vis spectroscopy, GPC, and DSC. The structure of EO polymers were varied by both side pendants and hydrocarbon spacer in order to study their effects on thermal stability and physical properties, which is extremely significant characteristics for device fabrication. The UV-Vis spectra also showed that NDI-based EO polymers did not decompose during polymerisation *via* ROMP. This could be used to confirm that the condition of ROMP using G3 as an initiator is appropriate for EO chromophore. In perspective of synthesis, NDI-based EO polymer can be advantageous over PMMA because of less process required to complete side-chain EO polymer. Moreover, the purification for poly(NDI)s by simple precipitation, is relatively less solvent consuming in comparison with PMMA-based EO polymer. This has potentially represented the possibility of large-scale EO polymer synthesis for industrial.

NDI based EO polymers, as expected, showed excellent Tg depending side chains and incorporated hydrocarbon spacer between NDI backbone and EO chromophore. However,

FTC chromophore used for this study has decomposition temperature at 210°C. Therefore, the selection of EO polymers for performance measurement would be carefully investigated.

For waveguide fabrication, the selection of suitable EO polymer will be primarily based on the loading density of EO chromophore, glass transition temperature, and molecular weight. This is to balance the dissolving capability in solvents, thermal stability, and EO polymer film quality, respectively.

Bibliography

[1]   N. S. Allen, Photochemistry and Photophysics of Polymer Materials, A John Wiley & Sons, Inc., Publication.

[2]   H. Ma, A. K.-Y. Jen, and L. R. Dalton, "Polymer-Based Optical Waveguides: Materials, Processing, and Devices," *Advanced Materials,* vol. 14, no. 19, pp. 1339-1365, 2002.

[3]   L. R. Dalton, W. H. Steier, B. H. Robinson, C. Zhang, A. Ren, S. Garner, A. Chen, T. Londergan, L. Irwin, B. Carlson, L. Fifield, G. Phelan, C. Kincaid, J. Amend and A. K.-Y. Jen, "From Molecules to Opto-Chips: Organic Electro-optic Materials," *Journal of Materials Chemistry,* vol. 9, pp. 1905-1920, 1999.

[4]   R. R. Barto Jr., C. W. Frank, P. V. Bedworth, S. Ermer, and R. E. Taylor, "Near-Infrared Optical Absorption Behavior in High-â Nonlinear Optical Chromophore-Polymer Guest-Host Materials. 1. Continuum Dielectric Effects in Polycarbonate Hosts," *The Journal of Physical Chemistry B,* vol. 108, no. 25, pp. 8702-8715, 2004.

[5]   Y.- J. Cheng, J. Luo, S. Hau, D. H. Bale, T.-D. Kim, Z. Shi, D. B. Lao, N. M. Tucker, Y. Tian, L. R. Dalton, P. J. Reid, and A. K.-Y. Jen, "Large Electro-optic Activity and Enhanced Thermal Stability from Diarylaminophenyl-Containing High-β Nonlinear Optical Chromophores," *Chemistrys of Materials,* vol. 19, no. 5, pp. 1154-1163, 2007.

[6]   G. R. Meredith, J. G. VanDusen and D. J. Williams, "Optical and nonlinear optical characterization of molecularly doped thermotropic liquid crystalline polymers," *Macromolecules,* vol. 15, no. 5, pp. 1385-1389, 1982.

[7]   M. He, T. Leslie, S. Garner, M. DeRosa, and J. Cites, "Synthesis of New Electrooptic Chromophores and Their Structure-Property Relationship," *The Journal of Physical Chemistry B,* vol. 108, no. 25, pp. 8731-8736, 2004.

[8] S. M. Garner, J. S. Cites, M. He, and J. Wang, "Polysulfone as an Electro-optic Polymer Host Material," *Applied Physics Letters,* vol. 84, pp. 1049-1051, 2004.

[9] I. Teraoka, D. Jungbauer, B. Reck, D.-Y. Yoon, R. Twieg, C. G. Willson, "Stability of nonlinear optical characteristics and dielectric relaxations of poled amorphous polymers with mainchain chromophores," *Journal of Applied Physics,* vol. 69, pp. 2568-2576, 1991.

[10] L. R. Dalton, A. W. Harper, R. Ghosn, W. H. Steier, M. Ziari, H. Fetterman, Y. Shi, R. V. Mustacich, A. K.-Y. Jen, K. J. Shea, "Synthesis and Processing of Improved Organic Second-Order Nonlinear Optical Materials for Applications in Photonics," *Chemistry of Materials,* vol. 7, pp. 1060-1081, 1995.

[11] M. Haller, J. Luo, H. Li, T.-D. Kim, Y. Liao, B. H. Robinson, L. R. Dalton, and A. K.-Y. Jen, "A Novel Lattice-Hardening Process To Achieve Highly Efficient and Thermally Stable Nonlinear Optical Polymers," *Macromolecules,* vol. 37, no. 3, pp. 688-690, 2004.

[12] O. K. A. Iobal, "Determination of Electro-optic Tensor Coefficeints of Organic Thin Film Using Fabry-Parot Interferometer Setup," KTH Information and Communication Technology, 2013.

[13] C.-C. Chang, C.-P. Chen, C.-C. Chou, W.-J. Kuo, and R.-J. Jeng, "Polymers for Electro-Optical Modulation," *Journal of Macromolecular Science, Part C: Polymer Reviews,* vol. 45, pp. 125-170, 2005.

[14] D. M. Burland, R. D. Miller, and C. A. Walsh, "Second-order nonlinearity in poled-polymer systems," *Chemical Reviews,* vol. 94, no. 1, pp. 31-75, 1994.

[15] M. H. Davey, V. Y. Lee, L.-M. Wu, C. R. Moylan, W. Volksen, A. Knoesen, R. D. Miller, and T. J. Marks, "Ultrahigh-Temperature Polymers for Second-Order Nonlinear Optics.

Synthesis and Properties of Robust, Processable, Chromophore-Embedded Polyimides," *Chemistry of Materials,* vol. 12, no. 6, pp. 1679-1693, 2000.

[16] J.-Y. Do, S.-K. Park, J.-J. Ju, S. Park, and M.-H. Lee, "Improved Electro-Optic Effect by Hyperbranched Chromophore Structures in Side-Chain Polyimide," *Macromolecular Chemistry and Physics,* vol. 204, pp. 410-416, 2003.

[17] H. Miura, F. Qiu, A. M. Spring, T. Kashino, T. Kikuchi, M. Ozawa, H. Nawata, K. Odoi, and S. Yokoyama, "High Thermal Stability 40 GHz Electro-optic Polymer Modulator," *Optic Express,* vol. 25, pp. 28643-28649, 2017.

[18] H. Sato, H. Miura, F. Qiu, A. M. Spring, T. Kashino, T. Kikuchi, M. Ozawa, H. Nawata, K. Odoi, and S. Yokoyama, "Low Driving Voltage Mach-Zehnder Interference Modulator Constructed From an Electro-optic Polymer on Ultra-thin Silicon with a Broadband Operation," *Optics Express,* vol. 25, pp. 768-775, 2017.

[19] J. Asrar, "Metathesis Polymerization of N-Phenylnorbornenedicarboximide," *Macromolecules,* vol. 25, pp. 5150-5156, 1992.

[20] J. Asrar and J. B. Hurlbut, "Synthesis, Rheology, and Physical Properties of a Metathesis Polymer," *Journal of Applied Polymer Sciences,* vol. 50, pp. 1727-1732, 1993.

[21] R. H. Grubbs, "Olefin-Metathesis Catalysts for the Preparation of Molecules and Materials (Nobel Lecture)**," *Angewandte Chemie International Edition,* vol. 45, pp. 3760-3765, 2006.

[22] M. S. Sanford, J. A. Love, and R. H. Grubbs, "Mechanism and Activity of Ruthenium Olefin Metathesis Catalysts," *Journal of the American Chemical Society,* vol. 123, pp. 6543-6554, 2001.

[23] J. Vargas, A. A. Santiago, R. Gavino A. M. Cerda, and M. A. Tlenkopatchev, "Synthesis and ring-opening metathesis polymerization (ROMP) of new N-fluoro-

phenylnorbornene dicarboximide by 2nd generation ruthenium alkylidene catalyst," *eXPRESS Polymer Letters,* vol. 1, pp. 274-282, 2007.

[24] D. J. Nelson, S. Manzini, C. A. Urbina-Blanco, and S. P. Nolan, "Key processes in ruthenium-catalysed olefin metathesis," *Chemical Communications,* vol. 50, pp. 10355-10375, 2014.

[25] A. J. Teator and C. W. Bielawski, "Remote control grubbs catalysts that modulate ring-opening metathesis polymerizations," *Journal of Polymer Science Part A, Polymer Chemistry,* no. 55, pp. 2949-2960, 2017.

[26] T. P. Montgomery, A. M. Johns and R. H. Grubbs, "Recent Advancements in Stereoselective Olefin Metathesis Using Ruthenium Catalysts," *Catalysts,* vol. 6, no. 87, 2016.

[27] I. Choinopoulos, "Grubbs' and Schrock's Catalysts, Ring Opening Metathesis Polymerization and Molecular Brushes—Synthesis, Characterization, Properties and Applications," *Polymers,* vol. 11, no. 298, 2019.

[28] A. M. Spring, F. Qiu, J. Hong, A. Bannaron, and S. Yokoyama, "Electro-optic properties of a side chain poly(norbornenedicarboximide) system with an appended phenyl vinylene thiophene chromophore," *Polymer,* vol. 119, pp. 13-27, 2017.

[29] X. Piao, X. Zhang, Y. Mori, M. Koishi, A. Nakaya, S. Inoue, I. Aoki, A. Otomo, and S. Yokoyama, "Nonlinear Optical Side-Chain Polymers Post-Functionalized with High-b Chromophores Exhibiting Large Electro-Optic Property," *Journal of Polymer Science: Part A: Polymer Chemistry,* vol. 49, pp. 47-54, 2011.

CHAPTER IV

Measurement of *in-situ* r$_{33}$ and fabrication Poly(NDI) Based EO Modulator

This chapter describes through whole processes for device fabrication in order to obtain EO polymer-based modulator. We also discuss the relation between the concentration of the novel NDI polymer-based solution and fabrication condition. The performance results of the complete EO modulators will be also discussed here.

4.1 Role of EO modulator in optical communication system
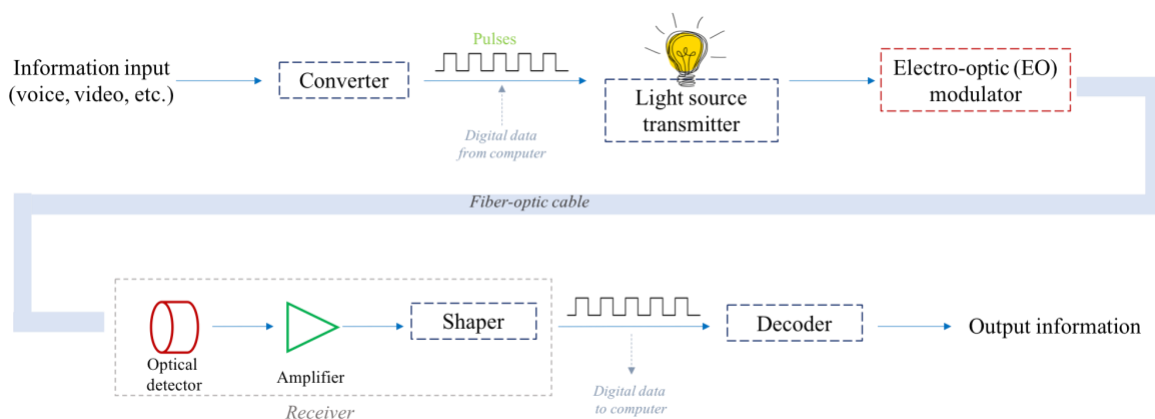
Figure 4.1 Basic block diagram of optical communication system

For data transmission in gigabits and beyond, fiber optic communication or telecommunication is the ideal alternative. Telecommunication system uses light wave technology to transmit data over distance through fibers by converting electrical signal into light. This type of communication system has been the major building block in any telecommunication

infrastructure, since it offers large bandwidth, light weight, long distance transmission, low attenuation, as well as, transmission reliability.

The data is input in form of electrical signal, and then is given to transmitter to convert them into optical signal. Here, light is modulated to carry information and coupled onto an optical fiber before being propagated by fiber optic cable over distances. Then, the optical signal is detected by optical detector and processed by amplifier to restore distorted optical signal in receiver circuitry. Subsequently, the data is translated back to the original electric signal as an output (see **Figure 4.1**).

The use of EO modulator for encoding electric data signals onto optical signal is one of approaches to overcome bandwidth limitation for future generation communication. The key challenge is the rate of light modulation. Moreover, new generation modulator is expected to be produced in mass scale and low cost, as well as high compatibility with any optical circuitry.

As discussed in Chapter I, organic EO polymers offer several advantages over typical crystal LiNbO$_3$. Especially, achievement in low velocity matching between RF and optical frequencies, that enable ultra-board bandwidth operation. This has led to exponential development in variety of EO polymers utilized for broadband light modulation. [1]-[8]

This thesis, we fabricated polymer-based EO modulator utilizing simple Mach-Zehnder interferometer (MZI) prototype. An input light travels along the waveguide structure, before splits into two arms which each path has a phase shift of 2π. During the waves travelling, interferences in constructive and deconstructive occur by polymer-based EO modulator.

According to **Eq.** (1-20) in Chapter 1 as shown;

$$V_\pi = \frac{\lambda d}{2\eta^3 r_{33} L\Gamma} \tag{1-20}$$

Half-wave voltage (V_π) is one of the most important characteristics of EO modulator. It implies the applied voltage needed to induce phase shift in a Mach-Zehnder. For V_π, a lower value is desirable since this would cheapen cost of electronics, as well as drastically reduce power consumption of modulator.

4.2 Optimization of suitable solvent for NDI-based EO polymer for fabrication

Generally, PMMA-based EO polymer solution for spin-coating is prepared at concentration 10 wt% in cyclopentanone. However, since physical properties of poly(NDI)s are distinctly different, concentration as well as spin-coating rate were investigated to achieve the optimum film quality.

The general procedure to prepare EO polymer solution is to dissolve calculated amount of EO polymer in solvent, and 1wt% of high purity silica filled phenolic resin F-554 as a coating agent. The mixture is stirred ay 50°C for an hour, following by stirring at ambient temperature for overnight.

Properties Solvents	b.p. (°C)	Solubility	Colour change
Cyclopentanone	131	Poor	×
1,2-**dichloroethane**	83	Excellent	o
o-**dichlorobenzene**	180	Excellent	×

Table 4.1 Comparison of physical properties of 5 wt% NDI-based EO polymer in solvents

Solubility and colour behaviors of EO polymer in each solvent is summarised in **Table 4.1**. Each sample was identically prepared at 5 wt% of NDI based EO polymer. Although cyclopentanone has high thermal stability, unfortunately, the solubility towards NDI-based EO polymer was relatively poor. On the other hand, EO polymer in *1,2*-dichloroethane possessed change in colour due to decomposition of EO chromophore. Whereas in this particular condition, *o*-dichlorobenzene demonstrated relatively better properties in both solubility and stability among others. The thermal stability of NDI polymer in *o*-dichlorobenzene was then further investigated.
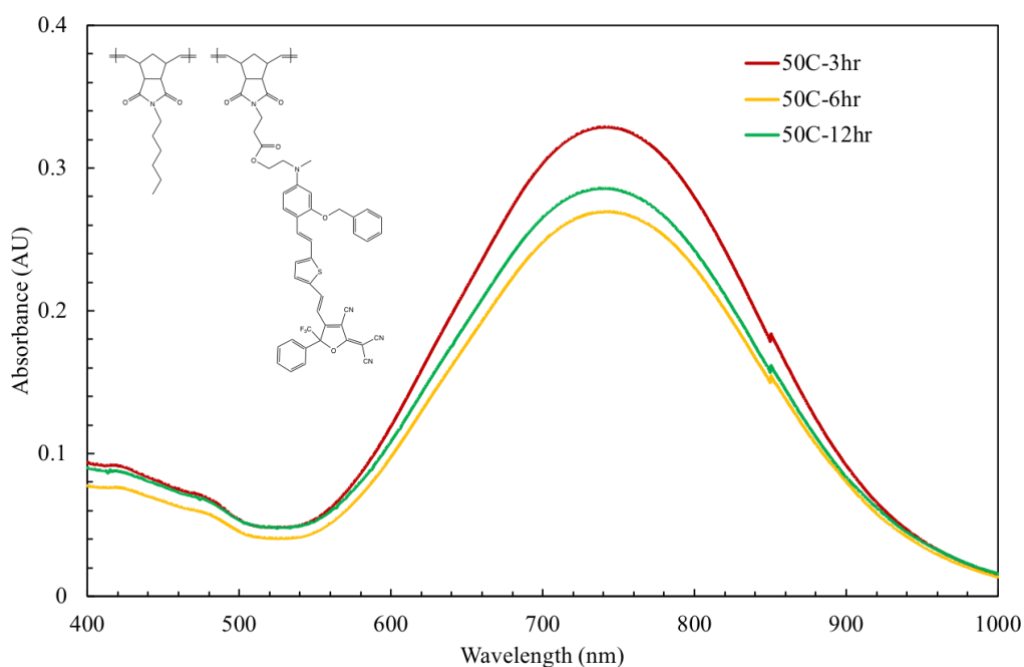
Figure 4.2 UV-Vis spectra of NDI polymer at 50°C for 3, 6, and 12 hours

To study the stability of *o*-dichlorobenzene towards NDI polymer, polymer solutions were heated at 50°C for 3, 6, and 12 hours. Each solution was diluted in THF for measurement of UV-Vis spectroscopy. As a result, UV-Vis spectra of NDI EO polymer in **Figure 4.2** did not show significant wavelength shift after heating up to 12 hours. This could confirm that

decomposition of EO chromophore did not occur. Thus, the use of o-dichlorobenzene is potentially applicable for preparation of NDI-based EO polymer.

4.3 Measurement of *in-situ* r_{33} by Teng-Man technique

4.3.1 Thin film preparation on ITO/glass substrates

The 10 wt% NDI based EO polymer was dissolved in o-dichlorobenzene, and stirred at ambient temperature for at least 12 hours. After the polymers were filtered through 0.2-0.45 μm filter, the solution was spin-coated onto ITO/glass substrate by spin-coating rate of 800 - 1000 rpm depending on viscosity of the solution for 30 seconds, following by baking at 95°C for 1 hour and 105°C under vacuum for 24 hours. Finally, Au layer was sputtered onto the film as an electrode by magnetron sputter. The EO polymer films on ITO/glass were then poled by heating up the temperature as close as their T_g. The electric field 50 V/μm was applied to top and bottom electrode as shown in **Figure 4.3**, following by cooling the temperature to freeze the alignment.
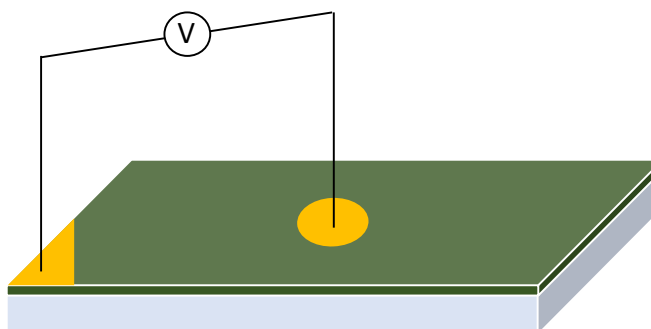
Figure 4.3 Poling setup for EO polymer film on ITO/glass substrate

4.3.2 Measurement of in-situ r_{33}

Polymer	Cr loading density (wt%)	Film thickness (μm)	T_{Poling} (°C)	V_{Poling} (V)	r_{33} (pm/V)
P-(1)	22	0.98	180	50	6.01
			185		5.91
			190		4.76
			195		1.22
P-(5)	21	0.99	180	50	6.89
			185		5.90
			190		5.03
			195		0.63
P-(6)	24	1.01	180	50	6.41
			185		9.91
			190		3.57
			195		4.33
P-(7)	24	2.10	150	50	6.49
			150	100	8.34
			150	150	8.11
P-(9)	26	2.51	160	50	8.34
			160	100	9.94
			160	150	4.66

Table 4.2 Summary of *in-situ* r_{33} for NDI based EO polymers by Teng-Man technique

EO polymer solutions were prepared in 10 wt% in *o*-dichlorobenzene. Unfortunately, gel formation occurred with **P-(2)**-**P-(4)**, **P-(8)** and **P-(10)**. Although the concentration was reduced into 7 wt%, it showed poor film quality which resulted in current shock while application of strong DC field. Therefore, they were excluded from the measurement. Summary of poling voltage (V_P), poling temperature (T_P), as well as film thickness of each

sample was concluded in **Table 4.2**. Film thickness was measured by surface profiler (*surface profiler – DEKTAK3).*

For those EO polymers with T_g over 200°C, T_p were varied in between 180 to 195°C in order to observe an optimum poling temperature without causing EO chromophore decomposition (T_d of the FTC chromophore used in this thesis is 210°C). In **Figure 4.4** exhibits the relations of r_{33} and T_p of **P-(1)**, **P-(5)**, and **P-(6)**, when V_p was fixed at 50 V. These clearly showed that optimum poling temperature were 180°C for **P-(1)** and **P-(5)**, and 185°C for **P-(6)**. By poling at temperature over optimum T_p, resulted in tremendous reduction in r_{33}, which could attribute to partial decomposition of FTC chromophore, as the temperature is closer to its T_d.
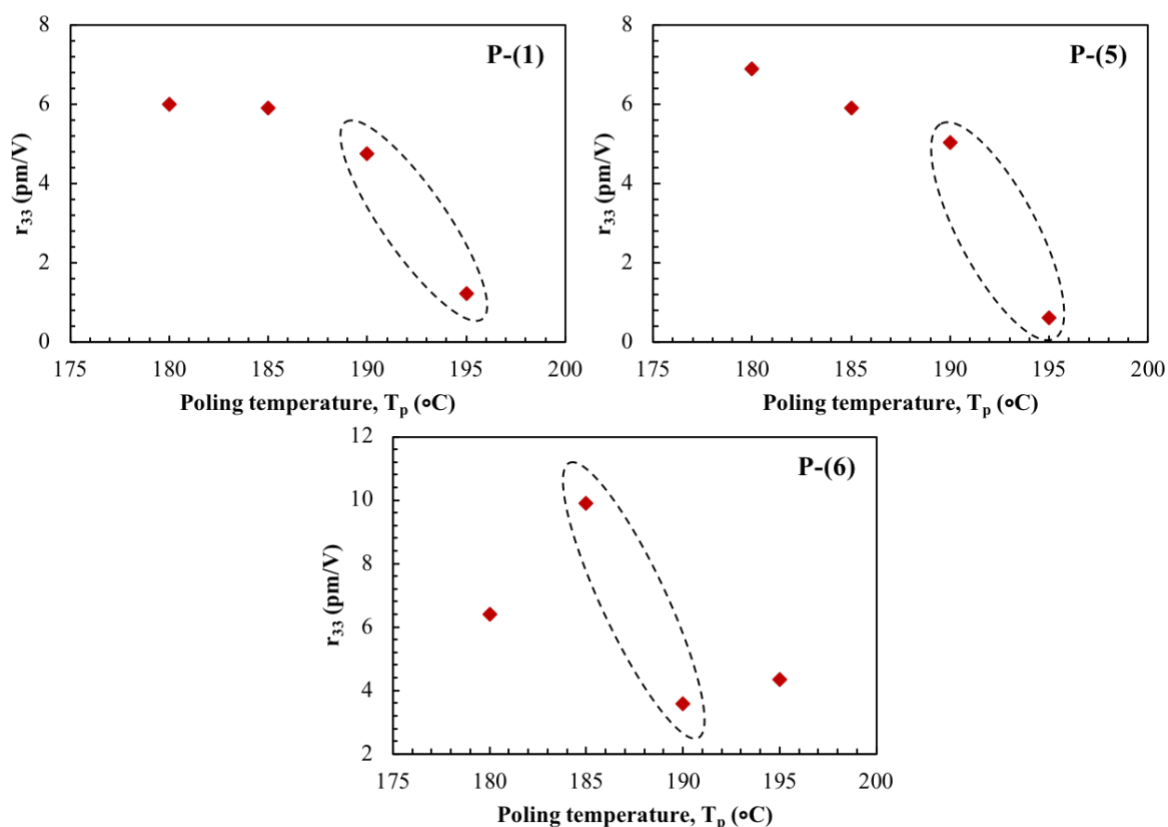
Figure 4.4 The relation between r33 and poling temperature, T_p of **P-(1)**, **P-(5)**, and **P-(6)** in which their T_g were unclear, when applied poling voltage, V_p was constant at 50 V

In the case of **P-(7)** and **P-(9)**, thanks to hydrocarbon pendant, they exhibited T_g below 200°C. These two polymers were then aimed to study the effect of poling voltage, V_p, where T_p were fixed at temperature close to their T_g. In general, for thin film on ITO/glass substrate, poling voltage is limited at 50 V/μm in order to prevent damage of the EO polymer. This obviously showed in the case of **P-(9)** in **Figure 4.5** as the voltage was risen to 150 V, r33 drastically reduced to 4.66 pm/V. This could be partially contributed to damage of the EO polymer itself.
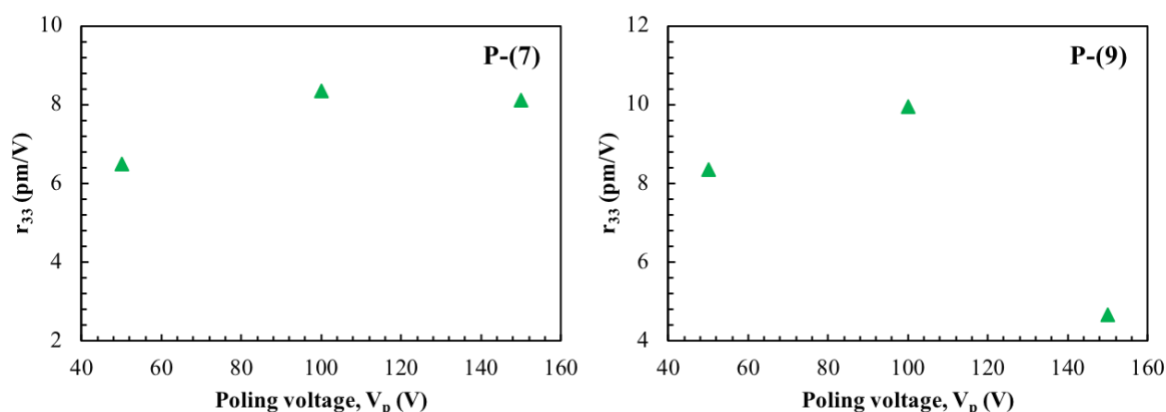
Figure 4.5 The relation between r_{33} and poling voltage, V_P of **P-(7)** and **P-(9)**, poling

temperature, T_P was at 150°C and 160°C, respectively

However, measured r_{33} were relatively low, although chromophore loading density in EO polymers were high. This is because high concentration of EO chromophore incorporated in NDI based EO polymers could cause shorter average distance between each dipolar molecule. This often resulted in strong dipole-dipole interaction between EO chromophores (as explained by **Eq. 1-19**, Chapter I). In Teng-Man method, the EO polymer is simply spin-coated onto ITO/glass substrate without protective layers, thus the application of the field for poling process is limited to prevent damage of materials. The restrictive voltage might not be sufficient to completely overcome dipole-dipole interaction of EO chromophore. Especially in side-chain polymer, in which when EO chromophore pendant could be strongly locked in polymer coils, limited freedom of rotation of EO chromophore. Thus, it was difficult to force the alignment much more than that of guest-host system.

4.4 Fabrication of NDI based EO modulator: silicon organic hybrid (SOH) modulator

In order to be able to apply stronger field which could surmount aggregation of EO chromophore, we selected the sample of NDI based EO polymer to be fabricated into EO

modulator waveguide. In this study, we fabricated silicon organic hybrid, so called SOH waveguide modulator.

Silicon photonics has explosively growth for decades due to its low-loss properties of silicon crystal in the near-infrared. Although it cannot provide nonlinearity due to its centrosymmetric structure, the innovative approach to integrate silicon with organic EO polymer, so called silicon organic hybrid (SOH) platform has promisingly enabled high performance hybrid integrated photonic devices, including optical interconnects, sensors and EO modulators. [9], [10], [11]

The integration between nonlinear optical polymers and silicon waveguides have proven highly efficient for new generation EO modulator. Since silicon has high index of refraction, it can provide tight optical confinement into a gap filled with EO polymer, which has lower refractive index. In addition, according to the structure of SOH modulator made by advance fabrication technology, half-wave voltage is also reduced with respect to the traditional EO modulator. Therefore, waveguide-based integrated optics have been widely employed as an ideal platform for concentrating and guiding light in nanoscale in a number of optical devices. [13]
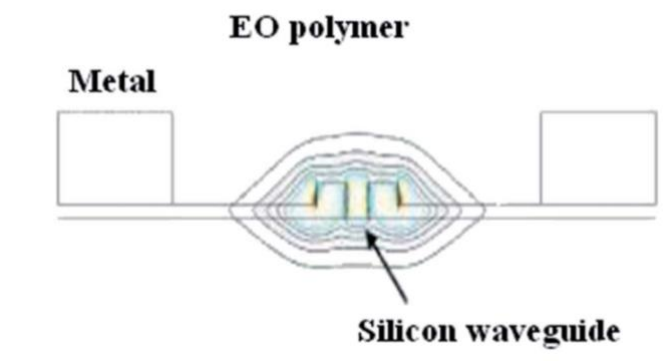
Figure 4.6 Structure and optical mode of SOH slot waveguide [12]

The fabrication of EO modulator (see **Figure 4.7**) was firstly proceeded by vacuum deposition of Al as a bottom electrode onto Si wafer. The solution of trimethylsilyl derivative in ethanol (sol-gel) was then spin-coated and baked at 120-140°C for 3-4 hours as a bottom cladding layer. After that, the adhesive layer *1,1,1,3,3,3*-hexamethyldisilazane (HMDS), and photoresist material S1813 was casted, following by waveguide patterning by electron beam (EB) lithography. The wafer was then developed by solution MF-319 and washed with distilled water. Then, the wafer was dry-etched by inductively coupled plasma etching (ICP; reactive ion etching (RIE), RIE-400iPB, SAMCO Inc.). The EO polymer **P-(7)** was then spin-coated onto the wafer, and was baked at 100°C under vacuum for overnight. The sol-gel solution was followingly casted to form top cladding film as a protective layer for the device. Au travelling-wave electrode was deposited from Au seed with titanium adhesive layer by vacuum evaporation. Finally, Au electrode was patterned by electroplating method using UV lithography.
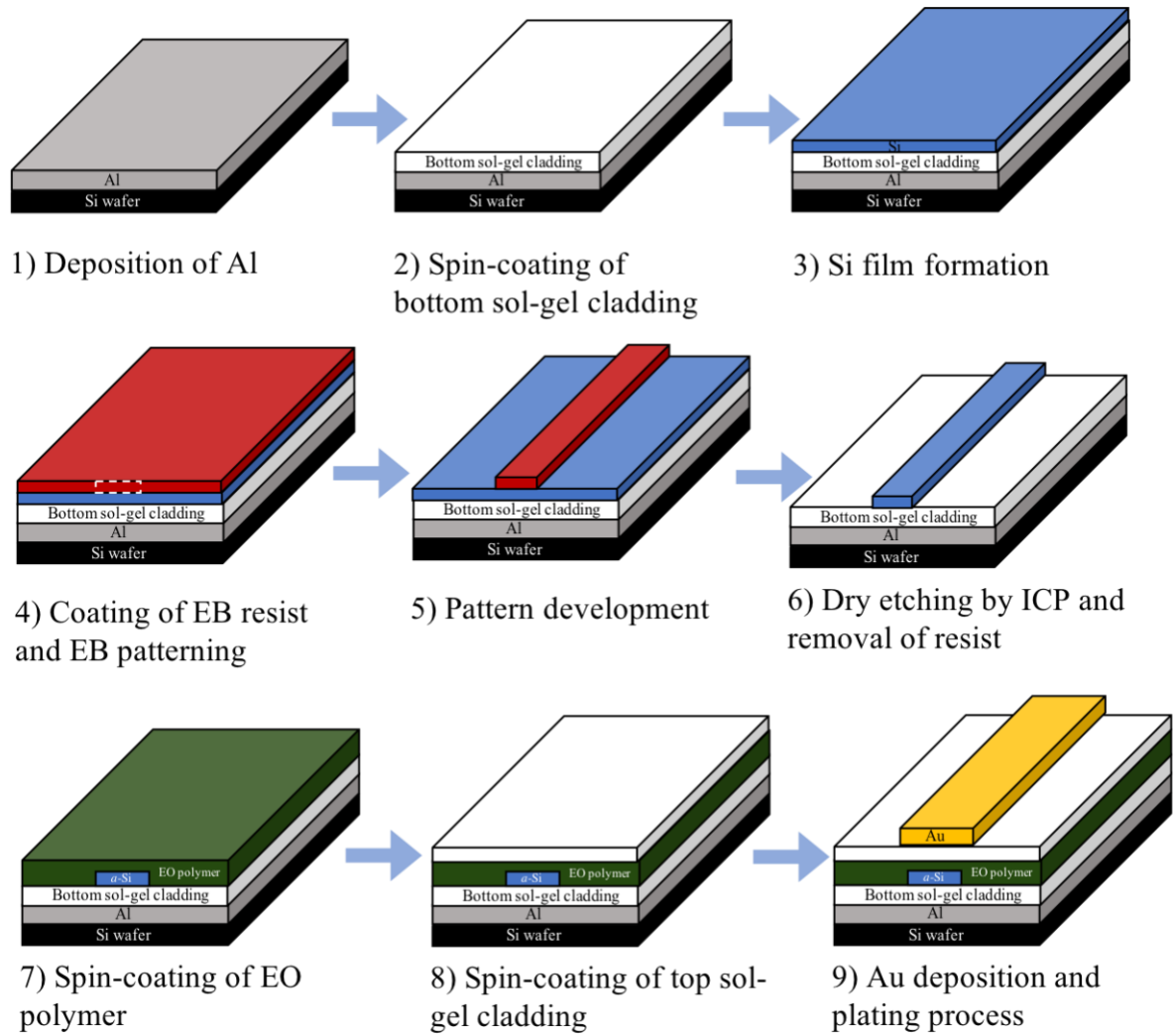
Figure 4.7 Fabrication process for EO polymer-based EO modulator with *a*-silicon 50 μm

thick and 3 μm wide
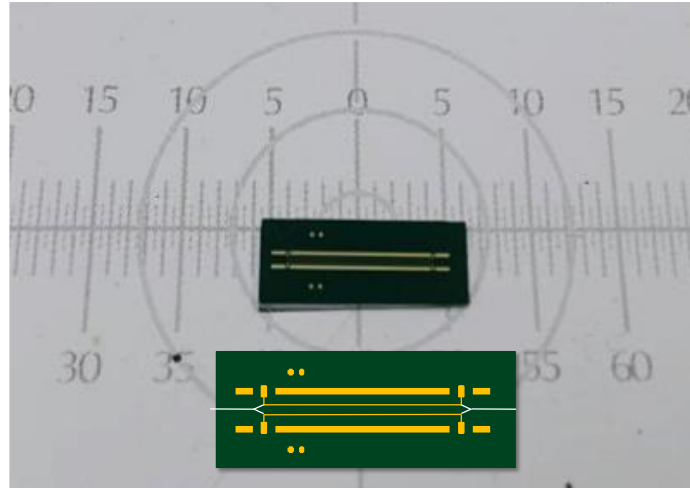
Figure 4.8 Schematic illustrator of top-view MZI waveguide modulator

and the width of EO polymer-based modulator which is approximately 8.0 mm

To realise second nonlinearity of modulator, the EO polymer waveguide was poled at poling temperature close to EO polymer's T_g. The EO polymer used for the particular fabrication was **P-(7)** which had well-balanced properties of 24 wt% of FTC chromophore, and its T_g was 151 °C. Thus, poling temperature for the EO modulator was at 150 °C. For waveguide modulator, sol-gel SiO_2 claddings are electric buffer layers having lower conductivity the EO polymer which can protect dielectric breakdown from poling at high voltage. Thus, the modulator was poled at 400 V. The set-up for push-pull poling process for waveguide was displayed in **Figure 4.9**.
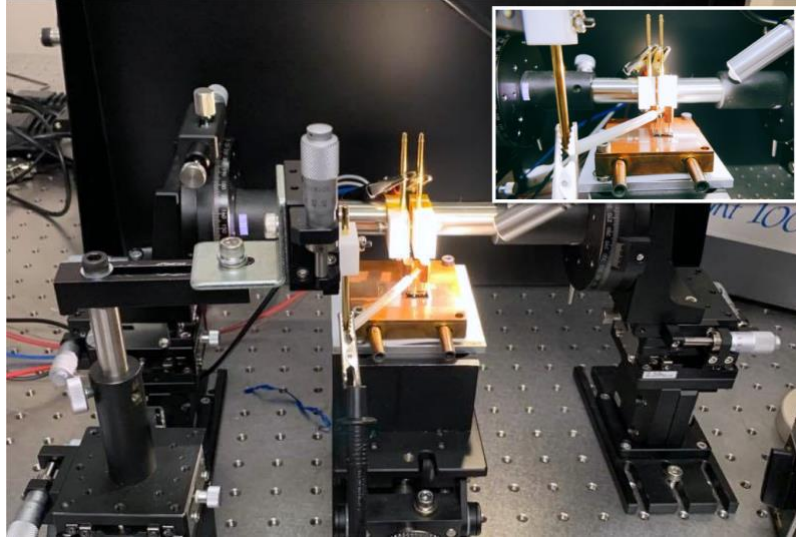
Figure 4.9 Push-pull poling process setup for waveguide modulator for alignment of dipole FTC chromophore in the direction of poling electric field V_p which is parallel to the optical field of transverse magnetic (TM) mode *(magnetic field does not involve in the direction of optical propagation)*

As mentioned, V_π is *in-device* EO coefficient which is an important parameter to evaluate modulation performance of EO modulator. The product of voltage-length, $V_\pi \cdot L$, was evaluated by using 10 kHz-frequency modulation. An input light at wavelength 1550 nm (81689A, Agilent) was coupled into the EO modulator as shown in **Figure 4.10** by polarized maintaining fiber in TM polarisation. Then the output light was collected and was channeled to photo-detector (PDA10CS, Thorlabs) by the fiber at another end. The differential voltages with triangle waveform from function generator (AFG1022, Tektronix) were then applied into two electrodes of the modulator.
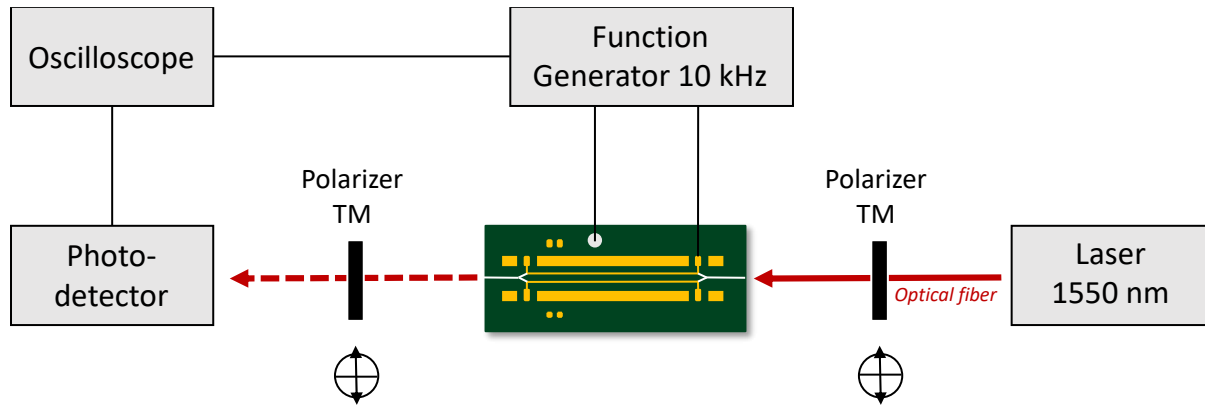
Figure 4.10 Measurement setup for π-voltage-length ($V_\pi \bullet L$) product for EO modulator

As explained by **Eq.** (1-20), V_π is influenced by electrode gap (d), interaction length of optical and electrical fields (*L*), and electrical-optical overlap integral (Γ). For the particular modulator, L was fabricated to be 8.0 mm long. Electrode gap, d, is 7.0 μm (bottom cladding was 3.0 μm, EO polymer was 1.0 μm, and top cladding was 1.0 μm). Electrical-optical overlap integral (Γ) was 74%. **Table 4.3** depicts the results of $V_\pi \bullet L$ product of EO modulator at different poling temperatures, and their estimate EO coefficients. As a result, we could achieve excellent $V_\pi \bullet L$ of 1.90 V•cm as the EO modulator was poled at 150°C, whereas the modulator poled at 140°C showed relatively larger $V_\pi \bullet L$ at 8.80 V. Therefore, the calculation of approximate r_{33} we could achieve over 200 pm/V. This confirmed that high poling efficiency could be achieved and thus resulted in low half-wave voltage for waveguide modulator made of NDI based EO polymer.

Poling temperature (°C)	$V_\pi \bullet L$ (V•cm)	V_π for 8.0 mm	r_{33} (pm/V)
140	8.80	7.04	60
150	1.90	1.52	222

Table 4.3 π-voltage-length products and estimated r_{33} of **P-(7)** at poling temperature 140°C and 150°C, where η is 1.63
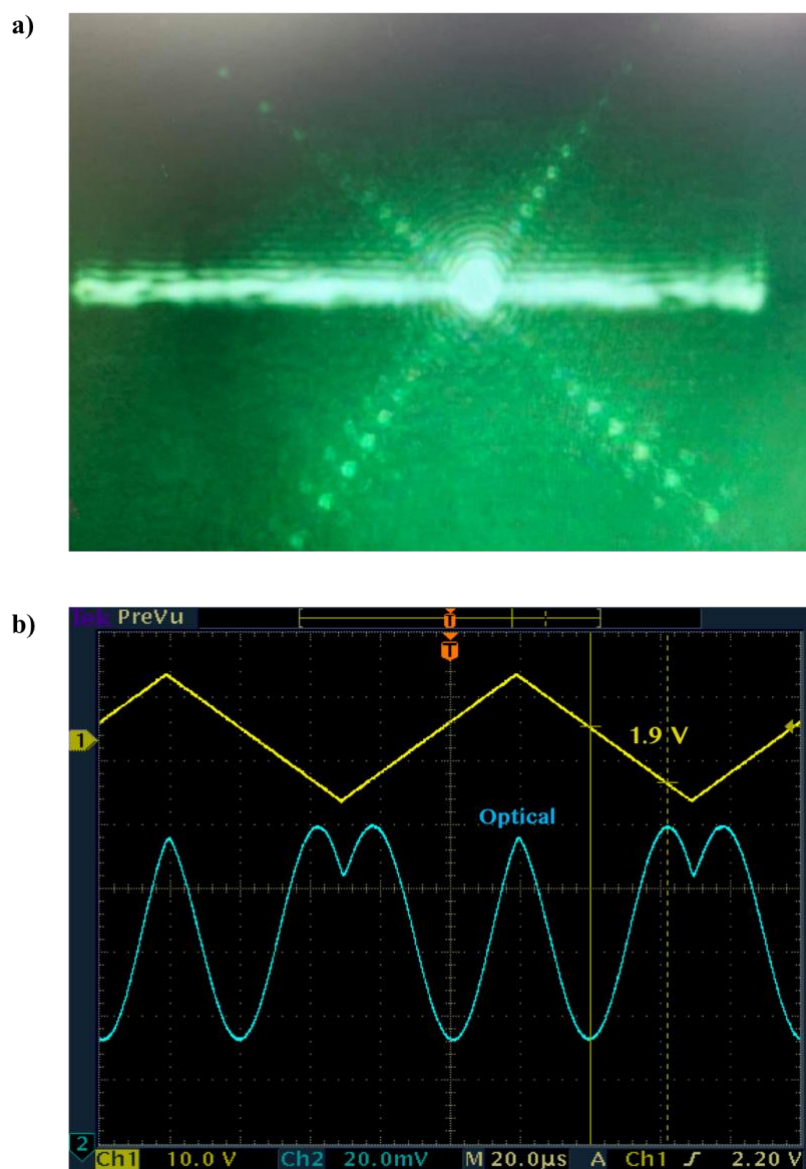
Figure 4.10 a) The image of optical profile mode and b) the measured transferred function of the modulator at 10 kHz of **P-(7)** at poling temperature of 150°C

4.5 Summary

This chapter firstly discussed about the solubility in organic solvents. EO polymer solution for fabrication is generally prepared in cyclopentanone or *1,2*-dichoroethane. However, we found poor solubility of NDI based EO polymer in cyclopentanone, especially in high loading density of FTC chromophore. Also, solution prepared in *1,2*-dichoroethane showed colour change, that could be attributed to decomposition of FTC chromophore that might cause reduction in EO

coefficient. Therefore, we purposed the use of *o*-dichlorobenzene which has high boiling point at 180°C. It was found that NDI based EO polymers showed the best solubility in *o*-dichlorobenzene without EO chromophore decomposition at 50°C for 12 hours. Therefore, *o*-dichlorobenzene was selected for dissolving EO polymers in this study. The measurement of *in-situ* r_{33} was investigated by Teng-Man reflection method. However, film quality and small applied voltage onto EO polymers on ITO/glass substrate for EO polymers with high chromophore concentration, significantly limited poling efficiency, which resulted in small r_{33}.

Larger applied voltage at 400 V could be applied to waveguide modulator due to sol-gel claddings as protective buffer layers. **P-(7)** was thus fabricated into EO modulator with *a*-Si as a core for optimal light concentration. EO polymer-based modulator was modulated with applied voltage with frequency 10 kHz, which resulted in small $V_\pi \cdot L$ at 1.9 V•cm, in which EO coefficient was approximately over 200 pm/V. This confirms that NDI-based EO polymer could provide promising half-wave voltage as a result of structural flexibility of EO polymer, which lead to high poling efficiency.

Bibliography

[1] C. C. Teng, "Traveling-wave polymeric optical intensity modulator with more than 40 GHz of 3-dB electrical bandwidth," *Applied Physics Letter,* vol. 60, pp. 1538-1540, 1992.

[2] D. Chen, H. R. Fetterman, A. Chen, W. H. Steier, L. R. Dalton, W. Wang, and Y. Shi, "Demonstration of 110 GHz electro-optic polymer modulators," *Applied Physics Letter,* vol. 70, pp. 3335-3337, 1997.

[3] M. Lee, H. E. Katz, C. Erben, D. M. Gill, P. Gopalan, J. D. Heber, and D. J. McGee, "Broadband Modulation of Light by Using an Electro-Optic Polymer," *SCIENCE,* vol. 298, pp. 1401-1403, 2002.

[4] X. Zhang, B. Lee, C.-Y. Lin, A. X. Wang, A. Hosseini, and R. T. Chen, "Highly Linear Broadband Optical Modulator Based on Electro-Optic Polymer," *IEEE Photonics Journal,* vol. 4, pp. 2214-2228, 2012.

[5] X.-L. Huang, C.-T. Li, P.-P. Dang, and C.-T. Zheng, "A Mach-Zehnder interferometer electro-optic switch with ultralow voltage-length product using poled-polymer/ silicon slot waveguide," *Optoelectronics Letters,* vol. 11, pp. 264-267, 2015.

[6] H. Chen, B. Chen, D. Huang, D. Jin, J. D. Luo, A. K.-Y. Jen, and R. Dinu, "Broadband electro-optic polymer modulators with high electro-optic activity and low poling induced optical loss," *Applied Physics Letters,* vol. 93, 2008.

[7] J. Luo, S. Huang, Y.-J. Cheng, T.-D. Kim, Z. Ssji, X.-H. Zhou, and A. K.-Y. Jen, "Phenyltetraene-Based Nonlinear Optical Chromophores with Enhanced Chemical Stability and Electrooptic Activity," Organic Letters, vol. 9, no. 22, pp. 4471-4474, 2007.

[8] Y. Enami, C. T. DeRose, C. Loychik, D. Mathine, R. A. Norwood, J. Luo, A. K.-Y. Jen, and N. Peyghambarian, "Low half-wave voltage and high electro-optic effect in hybrid

polymer/sol-gel waveguide modulators," Applied Physics Letters, vol. 89, p. 143506, 2006.

[9] M. Hochberg, T. Baehr-Jones, G. Wang, M. Shearn, K. Harvard, J. Luo, B. Chen, Z. Shi, R. Lawson, P. Sullivan, A. K.-Y. Jen, L. Dalton, and A. Scherer, "Terahertz all-optical modulation in a silicon–polymer hybrid system," Nature Materials, vol. 5, pp. 703-709, 2006.

[10] J. Leuthold, C. Koos, W. Freude, L. Alloatti, R. Palmer, D. Korn, J. Pfeifle, M. Lauermann, R. Dinu, S. Wehrli, M. Jazbinsek, P. Gunter, M. Waldow, T. Wahlbrink, J. Bolten, H. Kurz, M. Fournier, J.-M. Fedeli, H. Yu, and W. Bogaerts, "Silicon-Organic Hybrid Electro-Optical Devices," IEEE Journal of Selected Topic in Quantum Electronics, vol. 19, 2013.

[11] X. Zhang, C.-J. Chung, A. Hosseini, H. Subbaraman, J. Luo, A. K.-Y. Jen, R. L. Nelson, C. Y.-C. Lee, and R. T. Chen, "High Performance Optical Modulator Based on Electro-Optic Polymer Filled Silicon Slot Photonic Crystal Waveguide," Journal of LIghtwave Technology, vol. 34, pp. 2941-2951, 2016.

[12] J. Liu, G. Xu, F. Liu, I. Kityx, X. Liu, and Z. Zhen, "Recent advances in polymer electro-optic modulators," Royal Society of Chemistry, vol. 5, pp. 15784-15794, 2015.

[13] T. W. Baehr-Jones and M. J. Hochberg, "Polymer Silicon Hybrid Systems: A Platform for Practical Nonlinear Optics," Journal of Physical Chemistry, vol. 112, pp. 8085-8090, 2008.

CHAPTER V

Thesis's summary

In this thesis, we firstly reviewed the basic theoretical backgrounds for the understanding of modulator for future generation telecommunication system which indeed requires ultra-fast response and broad bandwidth. It has been proven that EO polymers have been considered potential materials for high performance modulator due to several advantages over typical inorganic crystal $LiNbO_3$. In general, Poly(methylmethacrylate)s, PMMAs have been widely used as a polymer host among number of polymeric materials. However, to achieve final PMMA based EO polymer, post-polymerisation is used to avoid chromophore decomposition from radical polymerisation. This approach requires purification, dialysis, which is time- and solvent- consuming, and often results in low yield. To shorten synthetic steps and control molecular weight of EO polymer for better thermos-physical properties, we purposed the use of norbornene-dicarboximide (NDI) derivatives as polymer segment for novel EO polymers.

Thermos-physical characterizations of NDI based EO polymer in side-chain approach exhibits potential properties over PMMA, including high thermal stability and well-controlled molecular weight distribution. Furthermore, NDI based EO polymer was prepared only by one-pot synthesis that required simple purification and also resulted in high yield. This would be beneficial in several aspects for large synthetic production in industrial scale, for instance, organic waste and cost reduction, and shorter synthetic line. Moreover, as we fabricated NDI based EO polymer into SOH modulator, it also exhibited excellent modulation performance as $V_\pi \cdot L$ at 1.9 V$\cdot$cm was achieved. From this, we strongly believe that NDI based EO polymer

with different side-group can be potential alternative as polymeric materials to be used with EO chromophore as already made in PMMA.

Future perspective

For further development of NDI based EO polymer, we herein purpose future perspective in material point of view. Since norbornene based polymer preliminarily demonstrates potential ability to be used in EO application, molecular structure can also be modified to enhance both thermal-physical and optical properties. For instance, some NDI polymers exhibited difficulty to be poled, which could attribute to dense packing of EO chromophore within polymer coils. We attempted to increase the flexibility of the materials with hydrocarbon side group and spacer. However, alternative approach by utilizing open dicarboximide ring would be worthy to experiment as well. This could possibly improve of flexibility of EO polymer in side-chain system and thus expectedly enhance poling efficiency and result in smaller V_π.

Acknowledgement

I would like to express my sincere gratitude to Professor Shiyoshi Yokoyama for continuous support throughout my study in both Master and Ph.D. I deeply thank you for teaching me a lot of techniques and tips for my research. Thank you so much for your inspiring guidance, encouragement, and patience that indeed gave me positive energy every time we had discussion.

Besides, I would like to thank Andy, Assoc. Andrew Spring, for giving me useful comments and being supportive through my research progress. I also would like to deeply thank you Prof. Hirotsugu Kikuchi and Prof. Katsuhiko Tomooka, for grateful opportunities to do lab rotations, that I gained several valuable knowledges from different fields. Moreover, I would like to thank you Prof. Masayuki Takeuchi and Takai san, at NIMS, and Prof. Samuel Ifor, Pavlos, Kou san, and all colleagues, at University of St. Andrews for precious internship experiences. I have leant insightful works and also gained lots of delightful moments there.

I thank you my colleagues in Yokoyama lab for being friendly and patient as listening to my poor Japanese and trying to communicate with me, and for funny moments we had with a number of nomikai and delicious BBQ parties. Thank you, Sato san, for helping me with all entry sheets for job hunting and every helpful recommendation. Also, thank you Shingai san for assistances throughout my period in the lab.

My acknowledgement would not be completed if I did not mention these superhuman who always be with me, rise or fall, with wonderful source of laugh and happiness. Thank you, all my friends for always being so supportive for everything in my life. You have always made

my day. Thank you for always listening to me complaining random things in life and distracting me from negative feelings. I could have not pass through several obstacles without you guys.

Lastly, I would like to delicate this paragraph to the love of my life, my mum. Although you would not read this, but I do want to say it anyway. Thank you, mum, for always being there believing in me for every decision I have made. I know there were million times I was not a good girl, but you have always been supporting me in any aspect of my life. Thank you for trusting your girl.

With Love,

Alisa.